Int. J. Plant Sci. 182(6):490–507. 2021.
1058-5893/2021/18206-0006$15.00 DOI: 10.1086/714281

SPECIAL ISSUE—CELEBRATING WOMEN IN PALEOBOTANY

OVULATE CONES OF *SCHIZOLEPIDOPSIS EDIAE* SP. NOV. PROVIDE INSIGHTS INTO THE EVOLUTION OF PINACEAE

Kelly K. S. Matsunaga,[1,*] Patrick S. Herendeen,* Fabiany Herrera,* Niiden Ichinnorov,† Peter R. Crane,‡ and Gongle Shi§

*Chicago Botanic Garden, 1000 Lake Cook Road, Glencoe, Illinois 60022, USA; †Institute of Paleontology and Geology, Mongolian Academy of Sciences, PO Box 46/650, Ulaanbaatar 15160, Mongolia; ‡Oak Spring Garden Foundation, Oak Spring, Upperville, Virginia 20184, USA, and School of the Environment, Yale University, New Haven, Connecticut 06511, USA; and §State Key Laboratory of Palaeobiology and Stratigraphy, Nanjing Institute of Geology and Palaeontology, Center for Excellence in Life and Paleoenvironment, Chinese Academy of Sciences, 39 East Beijing Road, Nanjing 210008, China

Guest Editor: Patricia E. Ryberg

Premise of research. The extinct conifer genus *Schizolepidopsis* is characterized by deeply bilobed ovuliferous scales bearing two adaxial seeds. Although it is frequently placed in Pinaceae, the evidence for a close relationship with the family is mixed. Resolving the affinities of *Schizolepidopsis* has important implications for the age of Pinaceae because putative reports of the genus extend into the Late Permian. We describe a new species, *Schizolepidopsis ediae* sp. nov., based on specimens from the Lower Cretaceous of Mongolia and Inner Mongolia, China, that represent the first anatomically preserved occurrences of *Schizolepidopsis*.

Methodology. Specimens were studied using light microscopy, cellulose acetate peels, and X-ray micro–computed tomography. To test relationships between *Schizolepidopsis* and Pinaceae, we performed conifer-wide phylogenetic analyses that included 10 previously described fossil conifers using DNA sequence data and a new morphological matrix of ovulate reproductive characters. Analyses were performed using Bayesian total evidence and parsimony backbone approaches.

Pivotal results. *Schizolepidopsis ediae* possesses key characters of Pinaceae, including those related to pollination biology. Most analyses placed *S. ediae* in crown group Pinaceae (abietoid clade), with all other *Schizolepidopsis* species forming a grade along the Pinaceae stem. Uncertainty in the data indicates that stem group affinities of *S. ediae* are also possible.

Conclusions. *Schizolepidopsis ediae* provides the first conclusive evidence linking *Schizolepidopsis* with extant Pinaceae. The phylogenetic relationships between extant Pinaceae and *Schizolepidopsis* suggest that seed wings evolved along the Pinaceae stem and not with the crown group and that, in combination with developmental genetic evidence, the simple ovuliferous scales of Pinaceae likely evolved from bilobed ovuliferous scales like those of *Schizolepidopsis*. More broadly, this study provides evidence of a Mesozoic Pinaceae stem group that might extend into the Paleozoic, helping to reconcile the ancient stem divergence of Pinaceae with its relatively recent crown age.

Keywords: paleobotany, fossil, conifer, Pinaceae, phylogenetics, evolution, ovuliferous scale.

Online enhancements: appendixes.

Introduction

Pinaceae are the largest family of conifers, comprising more than 200 species that are widespread throughout the Northern Hemisphere (Farjon 2017). Although they are usually resolved as the sister group to all other living conifers and thus their stem group should extend to the origin of crown conifers, Pinaceae appear relatively late in the conifer fossil record, and their origins remain enigmatic (Gernandt et al. 2018; Leslie et al. 2018). The unequivocal fossil record of Pinaceae begins in the Upper Jurassic (~157–152 Ma; Rothwell et al. 2012). High morphological diversity and an abundance of fossils in the Lower Cretaceous, as well as the first appearances of several extant genera (Blokhina and Afonin 2007; Klymiuk and Stockey 2012; Ryberg et al. 2012), suggest that Pinaceae underwent a rapid crown diversification

[1] Author for correspondence; current address: Department of Ecology and Evolutionary Biology, Biodiversity Institute, University of Kansas, 1200 Sunnyside Avenue, Lawrence, Kansas 66044, USA; email: matsunaga@ku.edu.

Manuscript received October 2020; revised manuscript received January 2021; electronically published May 10, 2021.

soon after their emergence in the geologic record (Smith and Stockey 2001; Smith et al. 2016). Molecular dating analyses indicate older clade ages overall, possibly a consequence of early rapid diversification (Leslie et al. 2018), but are nevertheless broadly consistent with the pattern observed in the fossil record. They estimate mean ages for the origin of the Pinaceae crown group in the Early Jurassic (~188 Ma) and divergence of the stem lineage in the late Carboniferous (~313 Ma), with long internal branches separating the diversification of living taxa and the deep backbone splits in the tree (Leslie et al. 2018). This pattern implies the persistence of Pinaceae stem lineages for more than 100 Myr before the divergence of the crown group. Indeed, the late Paleozoic and Mesozoic fossil record is rich in extinct conifers of uncertain phylogenetic affinities (Taylor et al. 2009). Although unambiguous Pinaceae are not known before the Late Jurassic, fossils of putative stem members of the family appear during the Triassic and possibly as early as the Late Permian (Delevoryas and Hope 1973; Taylor et al. 2009; Domogatskaya and Herman 2019).

Among the oldest of these possible Pinaceae stem lineages is the extinct genus *Schizolepidopsis* Doweld (formerly *Schizolepis* C.F.W. Braun), which comprises numerous species documented from localities throughout Eurasia (Rothwell et al. 2012; Domogatskaya and Herman 2019). The earliest records of *Schizolepidopsis* date to the middle to late Permian, with a handful of occurrences in the Triassic (Domogatskaya and Herman 2019). During the Jurassic, *Schizolepidopsis* was widespread throughout Eurasia, and it remained abundant through the Lower Cretaceous, when its distributions extended into Arctic latitudes (Domogatskaya and Herman 2019). No fossils of *Schizolepidopsis* are known from Upper Cretaceous strata, and the genus is presumed to have gone extinct sometime during the mid-Cretaceous (~100 Ma; Xu et al. 2013; Domogatskaya and Herman 2019).

Affinities with Pinaceae have been repeatedly proposed for *Schizolepidopsis* based primarily on ovule number and orientation (two inverted ovules per scale; Wang et al. 1997; Zhang et al. 2011; Leslie et al. 2013; Xu et al. 2013; Domogatskaya and Herman 2019). However, placement in Pinaceae is equivocal because most *Schizolepidopsis* species have lax cone structure, seed wings derived from the ovuliferous scale (which characterize living Pinaceae) have been observed in only a handful of species, and internal anatomy that might link *Schizolepidopsis* to Pinaceae is unknown (Rothwell et al. 2012; Leslie et al. 2013; Xu et al. 2013). Moreover, unlike living Pinaceae, *Schizolepidopsis* is characterized by having deeply lobed ovuliferous scales consisting of two distinct scale lobes bearing one seed each (hereafter, bilobed). This complex scale morphology is reminiscent of that of the extinct Voltziales (Meyen 1987; Wang et al. 1997), which had multilobed scales that are considered morphologically intermediate between the ovuliferous axillary shoots of the earliest conifers and the simple bract-scale complexes of living taxa (Florin 1954; Clement-Westerhof 1988; Stewart and Rothwell 1993; Taylor et al. 2009). *Schizolepidopsis*, therefore, exhibits traits of both Pinaceae and extinct conifer groups like Voltziales. Owing to the combination of characters present in *Schizolepidopsis* and the origins of the genus deep in geologic time, understanding the phylogenetic relationships of *Schizolepidopsis* could help to resolve gaps between the molecular and fossil ages of Pinaceae and further elucidate ovulate cone evolution in conifers.

We describe a new species of *Schizolepidopsis*, *S. ediae* Matsunaga, Herendeen, Herrera, Ichinnorov, Crane, et Shi, sp. nov., based on ovulate cones from the Early Cretaceous of Mongolia and China preserved as both lignitized compressions and siliceous permineralizations. This species is a new addition to a diverse conifer assemblage documented from the Early Cretaceous of Mongolia (Leslie et al. 2013; Shi et al. 2014; Herrera et al. 2015, 2016, 2017, 2020). The exceptional preservation of these fossils has facilitated observations of external morphology and internal anatomy at different developmental stages, providing insights into the natural history of this species. Moreover, the permineralized specimens represent the only known anatomically preserved *Schizolepidopsis* to date and yield unprecedented information on cone anatomy in the genus, which may be crucial for resolving evolutionary relationships. To understand the phylogenetic position of this species and the evolutionary origins of the genus *Schizolepidopsis*, we performed a series of phylogenetic analyses sampling all living conifer families, representatives of several extinct conifer groups, and three previously described *Schizolepidopsis* species. We discuss our observations and analytical results in the context of *Schizolepidopsis* taxonomy, developmental genetics, and morphological evolution.

Material and Methods

Locality and Age

Specimens of *Schizolepidopsis ediae* originate from one locality in Mongolia and another in Inner Mongolia, China. Cones preserved as lignitized compressions were collected from lignite seams of the Tevshiin Govi coal mine in Mongolia, located approximately 220 km south of Ulaanbaatar (lat. 45°58′54″N, long. 106°07′12″E). These deposits are part of the Tevshiin Govi Formation, which is most likely Aptian-Albian in age on the basis of palynostratigraphy (Ichinnorov 2003, 2005; Leslie et al. 2013; Herrera et al. 2016, 2017) and stratigraphic correlations (Graham et al. 2001; Erdenetsogt et al. 2009). Permineralized cones were recovered from chert horizons toward the base of a major coal-bearing unit at the Zhahanaoer opencast coal mine in Inner Mongolia, China (lat. 45°21′38.5″N, long. 119°25′04″E), which is part of the Lower Cretaceous Huolinhe Formation (Dong and Sun 2012; Xu et al. 2013; Li et al. 2016). The fossils from the Tevshiin Govi locality described in this article are housed in the paleobotanical collections of the Field Museum, Chicago (FMNH; collection numbers have the prefix PP). Additional specimens are also deposited in the Institute of Paleontology and Geology in Ulaanbaatar. The fossil specimens from the Zhahanaoer locality in Inner Mongolia are deposited in the paleobotanical collections of the Nanjing Institute of Geology and Palaeontology, Chinese Academy of Sciences (NIGPAS; collection numbers have the prefix PB).

Specimen Preparation and Study

Bulk lignite samples from Tevshiin Govi were disaggregated in soap and water, followed by dilute hydrogen peroxide (3%). Disaggregated organic material was sieved and panned using 125–500-μm sieves before air-drying. Selected mesofossils were then cleaned with hydrochloric and hydrofluoric acids. Chert specimens were studied using X-ray micro–computed tomography (μCT) and the cellulose acetate peel technique. We performed μCT scanning at the University of Michigan Computed Tomography in Earth and Environmental Sciences (CTEES) facility of

the Department of Earth and Environmental Sciences on a Nikon XT H 225 ST industrial μCT system equipped with a PerkinElmer 2000 X-ray detector panel and a tungsten reflection target. Specimens were scanned using 87–205 kV and 80–160 μA of X-ray power, depending on the specimen. Three-dimensional reconstructions and still images of μCT scans were produced using Avizo (FEI) and Mimics (Materialise) software. Cellulose acetate peels were produced following the technique of Joy et al. (1956), with the etching phase performed with full-strength hydrofluoric acid. Peels were subsequently mounted on glass slides in Canada balsam or Eukitt (O. Kindler, Freiburg, Germany) mounting medium for light microscopy and photography. Fossils were photographed using a Canon Rebel camera with a 100-mm macrolens attached to a Stackshot system at the Chicago Botanic Garden and a Nikon Eclipse LV100ND microscope with a DS-Fi3 camera system (Nikon Metrology) at the University of Kansas. Focal stacking of images was performed using Helicon Focus software (ver. 7.5.8 Pro; Helicon Soft). See appendix A (apps. A–D are available online) for scan parameters, CT videos, and surface files.

Phylogenetic Analyses

Taxon sampling. Phylogenetic analyses were performed using DNA sequence data and a new morphological matrix of ovulate reproductive characters. This matrix comprised 40 taxa, including representatives for all extant conifer families, 10 previously described fossil conifer species, *S. ediae*, and *Ginkgo biloba* (see app. B). Within Pinaceae, Araucariaceae, and Sciadopityaceae, one species per genus was sampled. For Cupressaceae, Taxaceae, and Podocarpaceae, exemplar species representing major clades within these families were sampled. Ten extinct species representing several seed plant groups were included in some analyses because taxa with novel character combinations can alter character distributions within the tree and thus influence the phylogenetic position of other taxa. By including them, we tested (1) whether the phylogenetic position of *S. ediae* is influenced by the inclusion of other fossils in the analysis and (2) the monophyly and pinaceous affinities of the genus *Schizolepidopsis*. These fossils were *Cordaixylon dumusum* Rothwell & Warner (Upper Pennsylvanian, Cordaitales; Rothwell 1993), *Hanskerpia hamiltonensis* Rothwell, Mapes & Hernandez-Castillo (Upper Pennsylvanian, Voltziales; Rothwell et al. 2005), *Emporia lockardii* Mapes & Rothwell (Pennsylvanian, Voltziales; Mapes and Rothwell 1984, 2003; Rothwell et al. 2005), *Telemachus aequatus* Yao, Taylor et Taylor (lower Middle Triassic, Voltziales; Yao et al. 1997; Bomfleur et al. 2013), *Voltzia hexagona* (Bischoff) Geinitz (Permian, Voltziales; scoring from Rothwell et al. 2005; Looy 2007), *Pararaucaria patagonica* Wieland (Middle Jurassic, Cheirolepidiaceae; Escapa et al. 2012), and *Eathiestrobus mackenziei* Rothwell, Mapes, Stockey et Hilton (Upper Jurassic, Pinaceae; Rothwell et al. 2012). We also included three previously described species of *Schizolepidopsis*: *S. canicularis* Leslie, Glasspool, Herendeen, Ichinnorov, Knopf, Takahashi, et Crane from the Lower Cretaceous Tevshiin Govi Formation of Mongolia (Leslie et al. 2013), *S. longipetiolus* Xu XH et Sun BN from the Lower Cretaceous Huolinhe Formation of Inner Mongolia, China (Xu et al. 2013), and *S. daohugouensis* Zhang, D'Rozario, Yao, Wu, et Wang from the Middle–Upper Jurassic Tiaojishan Formation of Inner Mongolia, China (Zhang et al. 2011).

Morphological matrix. The morphological matrix consists of 68 ovulate reproductive characters. Most of the characters were derived from previously published matrices that focused on individual conifer groups, including Voltziales (Rothwell et al. 2005), Podocarpaceae (Andruchow-Colombo et al. 2019), Araucariaceae (Escapa and Catalano 2013), Cupressaceae (Farjon 2005; Escapa et al. 2008), and Pinaceae (Smith et al. 2016; Gernandt et al. 2018). In some cases, character coding or scoring was altered from the original matrix to accommodate modified character definitions and to eliminate discrepancies between similar characters shared by different matrices. Additional data on the anatomy and morphology of extant and fossil taxa were obtained from the literature (Radais 1894; Carothers 1907; Owens and Blake 1983; Mapes and Rothwell 1984; Takaso and Tomlinson 1989, 1991, 1992; Tomlinson and Takaso 1989; Tomlinson 1992; Rothwell 1993; Owens et al. 1995, 1998; Runions et al. 1995; Takaso and Owens 1995; Mill et al. 2001; Farjon and Garcia 2002, 2003; Schulz and Stützel 2007; Hernandez-Castillo et al. 2009; Escapa et al. 2012; Jagel and Dörken 2014, 2015*a*, 2015*b*; Dörken and Nimsch 2015; Farjon 2017; Dörken and Rudall 2018). More generally, the matrix was designed to accommodate expanded taxon sampling of both extant and fossil seed plants in future analyses. For this reason, some characters are not phylogenetically informative with the current taxon sampling but were retained to enhance the utility of the data set for future studies focused on conifer or seed plant relationships. Character definitions, references for characters, and specific coding or scoring decisions can be found in the online appendixes and in the matrix nexus file (Mesquite formatted).

Like any morphological matrix, our character coding makes implicit assumptions about the homology of structures in fossils and living conifers. We follow the Florin model of ovulate cone evolution in conifers (Florin 1954) since it is the most comprehensive and broadly accepted model of homology across conifers (e.g., Gifford and Foster 1989). As such, we consider ovulate cones of living conifers as homologous with those of fossil conifers with compound ovuliferous shoots, wherein modern bract-scale complexes are derived by the reduction and modification of ovuliferous dwarf shoots and their subtending bracts. In extant Pinaceae and Sciadopityaceae, the bract and scale are morphologically distinct, but in other families, the homologies are less straightforward. We use the following interpretations of homology, which have been proposed by other researchers and used in previous phylogenetic reconstructions and which are supported by morphological and developmental studies. In Araucariaceae, the bract and scale are usually fused in a single unit, or the very tips of the bract and scale are free (e.g., *Araucaria* Juss.; Stockey 1982; Andruchow-Colombo et al. 2019). In Podocarpaceae, the ovuliferous scale is modified into an epimatium surrounding the seed, which is subtended by a bract that is sometimes fused with the axis and other bracts to form a fleshy receptacle (Mill et al. 2001), an interpretation supported by developmental morphology (Tomlinson et al. 1991; Tomlinson 1992) and genetics (Englund et al. 2011). In most Cupressaceae, developmental studies indicate that the ovuliferous scale is reduced down to either just the ovules or a small pad of tissue, and seeds are instead protected by the bract (Groth et al. 2011; Jagel and Dörken 2014, 2015*a*; Dörken and Rudall 2018). However, some taxodiaceous Cupressaceae, such as *Cryptomeria* and *Cunninghamia*, have a prominent lobed structure (sometimes referred to as "teeth") between the ovules and

bract that is often interpreted as the ovuliferous scale (e.g., Schulz and Stützel 2007). This interpretation is supported by examples of fossil Cupressaceae that have distinct lobed ovuliferous scale tissues (e.g., Rothwell et al. 2011; Spencer et al. 2015), but developmental genetic studies indicate that molecular markers of ovuliferous scale identity are absent in *Cryptomeria* teeth (Groth et al. 2011). Although we acknowledge that the evidence for homology is mixed, we tentatively treat the lobed tissue subtending the ovules in taxodiaceous Cupressaceae as homologous to the ovuliferous scale of other conifers. In Taxaceae, with the exception of *Cephalotaxus* Siebold & Zucc. ex Endl., ovulate cones are reduced down to a single ovule, which is surrounded by a fleshy aril. There is no developmental genetic evidence that the aril is homologous with the ovuliferous scale (Englund et al. 2011), and it is treated here as a novel structure.

Molecular matrix. The DNA sequence data were obtained from GenBank, and we primarily used markers and accessions sampled by Leslie et al. (2018). Four chloroplast and nuclear loci were used, as follows: *18s*, *rbcL*, *matK*, and *PHYP* (see app. C for GenBank accession numbers). Sequences were aligned using MAFFT (Katoh and Standley 2013) and were edited manually before the alignment edges were trimmed. The final alignment contained 8470 sites. We used PartitionFinder2 to evaluate competing partitioning schemes using the Akaike information criterion corrected for sample size under a greedy search algorithm (Lanfear et al. 2012, 2017). We opted to use the best-scoring partitioning scheme, which comprised 10 partitions and included codon partitioning for the coding regions.

Analyses. Phylogenetic analyses were performed to investigate the evolutionary relationships of *S. ediae*, with and without the inclusion of other fossils, and the relationships of genus *Schizolepidopsis* relative to Pinaceae. Total evidence analyses of the combined molecular and morphological data set were performed using a Bayesian approach in the program MrBayes, with a data set that included all fossil taxa and one in which *S. ediae* was the only fossil. Tree searches of the combined matrix in MrBayes were performed using two parallel runs of metropolis-coupled Markov chain Monte Carlo consisting of three hot and one cold chain, with chain length set to 10 million generations per run. Runs were sampled every 1000 generations, for a total of 10,000 sampled trees. The molecular data were analyzed using the best-scoring partitioning scheme, which included 10 partitions and a combination of GTR and SYM models (see app. D). The morphological partition was analyzed using the Mk model of morphological evolution, corrected for ascertainment bias, with gamma-distributed between-character rate variation. Each run was assessed visually in Tracer to ensure convergence and adequate effective sample sizes of all parameters. The sampled distribution of trees was summarized using a 50% majority-rule consensus criterion after the first 25% of trees were discarded as burn-in. All MrBayes analyses were performed on the CIPRES Science Gateway (Miller et al. 2010). See appendix D for input files and resulting tree files for all analyses.

In addition, we performed these same analyses with parsimony in PAUP (ver. 4.0a168; Swofford 2003) using the morphological data paired with a molecular backbone constraint. The backbone constraint was necessary because the sampled morphological characters alone do not recover the well-supported and widely accepted relationships among extant conifers, mostly because of the derived condition of cones in Taxaceae, which share few characters with other conifers. For the *S. ediae*–only analyses, tree searches were performed using 1000 random addition sequence replicates to generate starting trees followed by 1000 rearrangements using tree-bisection-reconnection as the branch-swapping algorithm. Node support was estimated using a full search of 100 bootstrap replicates following the same procedure. For the analysis with all fossils included, we used a similar procedure but increased the starting tree search to 10,000 random addition sequence replicates and set the rearrangement limit to 100,000 (see app. D for all settings used). This was to ensure adequate search of tree space, as we found the tree search to be sensitive to seed number at lower numbers of replicates and rearrangements. Because of the high number of most parsimonious trees (MPTs; $n = 84$), bootstrap analyses were not informative, and the results of this analysis were instead summarized using a 50% majority-rule consensus of all MPTs.

To evaluate competing equally parsimonious topologies, as well as suboptimal topologies obtained by bootstrap resampling of the *S. ediae*–only data set, we calculated likelihood scores and tree length in PAUP. Tree likelihoods were calculated allowing for gamma-distributed between-character rate variation, with the gamma shape parameter and proportion of invariant sites estimated from the data. We tested whether trees with higher likelihood scores were significantly different from trees with lower likelihood scores using one-tailed Shimodaira-Hasegawa tests with a resampling estimated log-likelihood (RELL) bootstrapping procedure in PAUP. This test was performed for the entire set of bootstrapped trees (for the *S. ediae*–only analysis) and for all MPTs (for the all fossils analysis). The backbone constraint tree was constructed with maximum likelihood in the program RAxML (Stamatakis 2014), using only the molecular data to avoid analytical circularity, and was analyzed using the general time-reversible model of nucleotide substitution with gamma-distributed among-site rate variation (GTR+G model) for a set of 10 partitions conforming to the best-scoring partitioning scheme.

Results

Systematics

Order—Pinales Gorozh. 1904

Family—Pinaceae Spreng. ex F.Rudolphi 1830

Genus—Schizolepidopsis *Doweld, 2001, emend. Domogatskaya et Herman*

Type Species—Schizolepidopsis liasokeuperianus *C.F.W. Braun 1847*

Species—Schizolepidopsis ediae *Matsunaga, Herendeen, Herrera, Ichinnorov, Crane, et Shi, sp. nov.*

Specific diagnosis. Ovulate cones compact, elongate, bearing helically arranged bract-scale complexes. Cone axis slender with parenchymatous pith surrounded by a continuous cylinder of secondary xylem; inner cortex with a single large circumferential resin cavity, outer cortex sclerenchymatous. Ovuliferous scales stalked, bilobed, with lobes diverging distal to seed body.

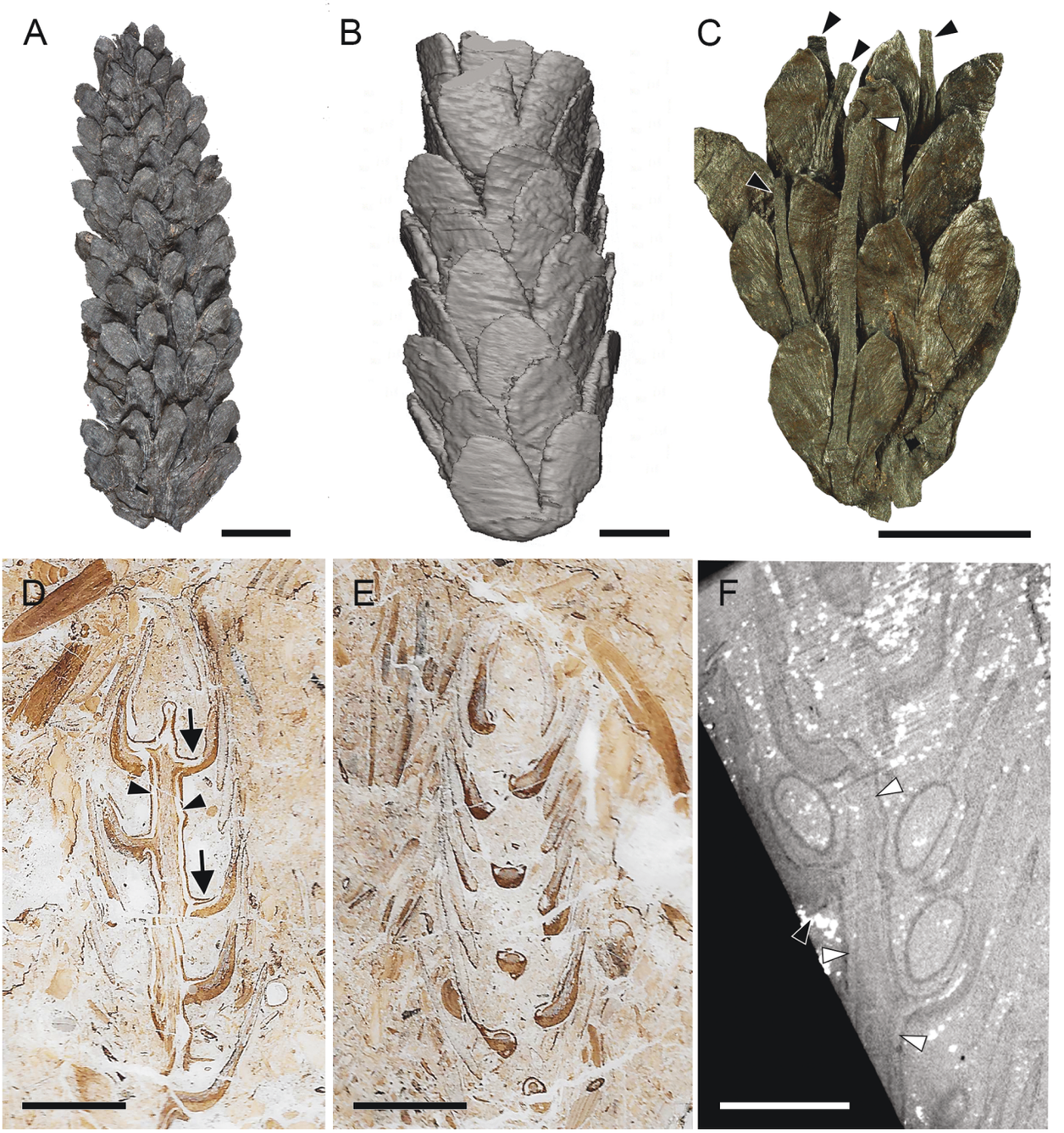

Fig. 1 Lignitized and permineralized ovulate cones of *Schizolepidopsis ediae* sp. nov. *A*, Apical fragment of a cone from compressed lignite. Note the variation of apex morphology, which ranges from rounded to short-acuminate, and that the ovuliferous scales decrease in size distally. PP59848. Scale bar = 5 mm. *B*, Three-dimensional rendering of a permineralized cone from a micro–computed tomography (μCT) scan. Note the similarity to cones preserved in lignite (*A*, *C*) in size and morphology. PB23506A. Scale bar = 3 mm. *C*, Cone fragment from compressed lignite with connected bracts (arrowheads). Note that the bracts are linear and exceed the length of the ovuliferous scale that they subtend. Most bracts shown are broken at the tip, but one is intact, with a short-acuminate apex (white arrowhead). PP59844. Scale bar = 5 mm. *D*, Longitudinal section of a cone lacking seeds. Note the divergence angles of the bract-scale complexes (arrows) and the wide cortical resin cavity (arrowheads; see fig. 3*A*–3*D* for details of the cortical resin cavity). PB23507, peel 1. Scale bar = 5 mm. *E*, Longitudinal tangential section of a cone lacking seeds. Note the stalks of the bract-scale complexes in transverse section (see fig. 3*D*, 3*E* for detail) and the dark color of the bract-scale complexes proximally and abaxially, indicating a greater concentration of sclerenchyma. PB23508, peel 4. Scale bar = 5 mm. *F*, Longitudinal section of a permineralized cone from a μCT scan. Note the presence of seeds and a resin cavity in the cone axis (white arrowheads) and the absence of bracts (broken base; black arrowhead). PB23506A. Scale bar = 5 mm.

Lobes widest medially, apexes rounded to short-acuminate. Scale supplied by a single large abaxially concave vascular bundle abaxial to a large curved resin canal; vascular bundle and resin canal branched within scale to supply each lobe. Bract linear, exceeding scale; sclerenchymatous basally with single round resin canal and vascular bundle of primary xylem. Vascular traces to bract and scale not united, with separate origins within cone axis. Resin canals of bract and scale with separate origins within cone axis. Bract and scale free for most of length, fused basally. Seeds two, rarely one, per scale, with distal wing derived from entire adaxial surface of each scale lobe; sclerotesta thin, sarcotesta parenchymatous, three or more cell layers thick. Seeds inverted, micropyles oriented toward cone axis, overhanging edge of ovuliferous scale. Micropyles with two micropylar arms. Seed body, micropylar arms, and scale bases densely trichomatous or papillate.

Holotype. PB23509 (figs. 2*B*, 4*A*–4*G*), Zhahanaoer coal mine, Inner Mongolia, China. Paleobotanical Collections, Nanjing Institute of Geology and Palaeontology, Chinese Academy of Sciences.

Other illustrated material. PB23506, PB23507, PB23508, PP59844, PP59845, PP59846, PP59847, PP59848.

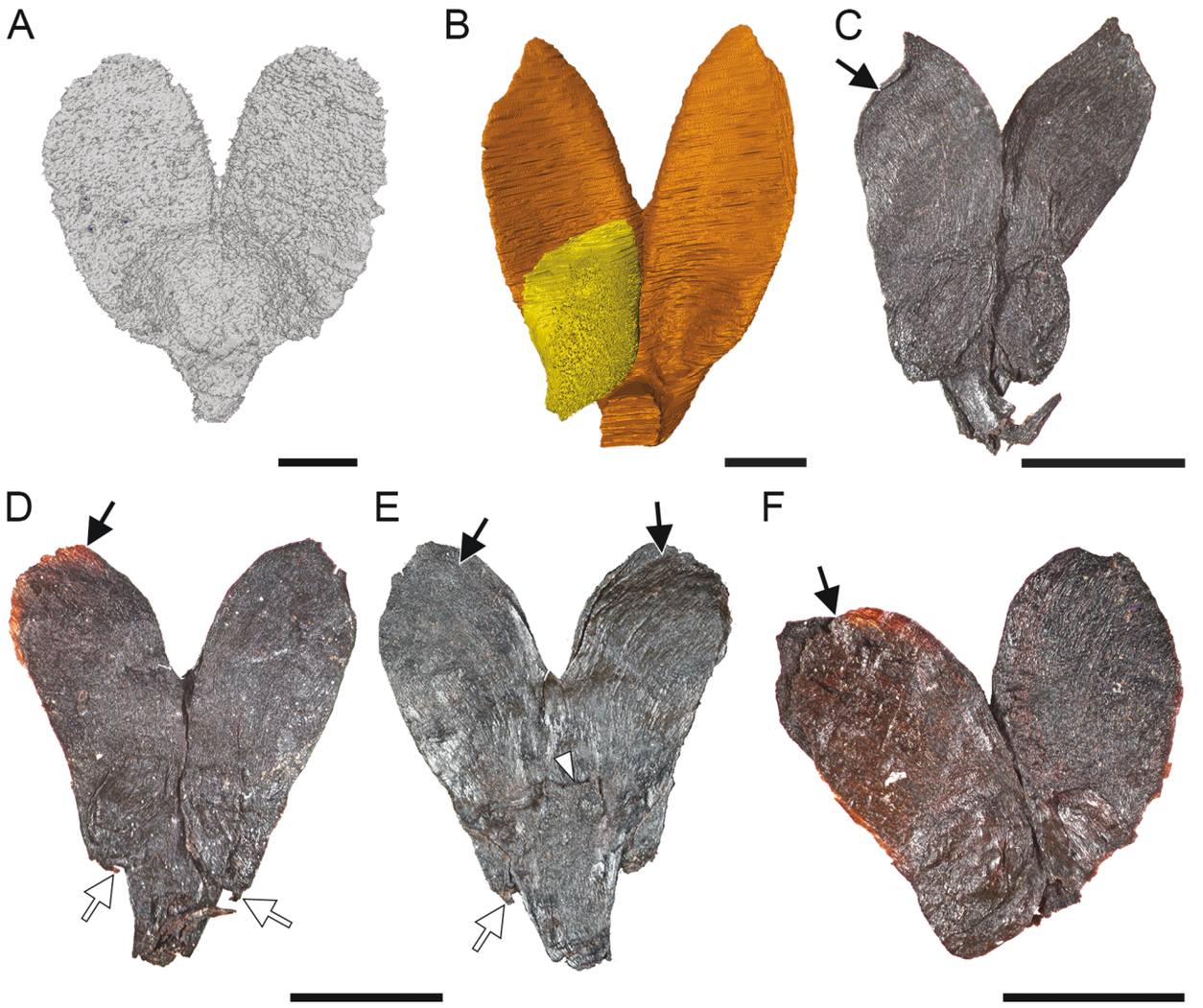

Fig. 2 Ovuliferous scales. *A*, Three-dimensional rendering of an ovuliferous scale based on a micro–computed tomography (μCT) scan of a permineralized specimen. Note the rounded apexes of the lobes, the similarity in size and shape compared with lignitized specimens (*D*–*F*), and the proximal depressions where seeds were positioned. PB23506. Scale bar = 2 mm. *B*, Three-dimensional rendering of an ovuliferous scale with seeds based on a μCT scan of a permineralized specimen. Only one seed is shown (yellow; *left*) to show the depression on the ovuliferous scale formed by the seed body (scale lobe; *right*). Note the short-acuminate apexes of the lobes, similar to those of the lignite specimen in *C*, and the divergence of the scale lobes above the seed body. Only the seed body and not the wing is shown in this rendering. PB23509, holotype. Scale bar = 5 mm. *C*, Ovuliferous scale with seeds preserved as a lignitized compression. Note the short-acuminate lobe apexes. The separation of the seed wing from the ovuliferous scale is visible at the distal end of one scale lobe (arrow) as a thin line. PP59847. Scale bar = 5 mm. *D*, *E*, Adaxial (*D*) and abaxial (*E*) sides of a lignitized ovuliferous scale with seeds. The seed wing is separated from the ovuliferous scale distally (black arrows), visible as a light brown region in *D*. Note the thin protruding micropyle on the proximal ends of the seeds (white arrows) and the scar left by a broken or abscised bract (arrowhead). PP59845. Scale bar = 2 mm. *F*, Lignitized ovuliferous scale with seeds, showing a seed wing partially detached from the ovuliferous scale lobes (arrow). PP59846. Scale bar = 2 mm.

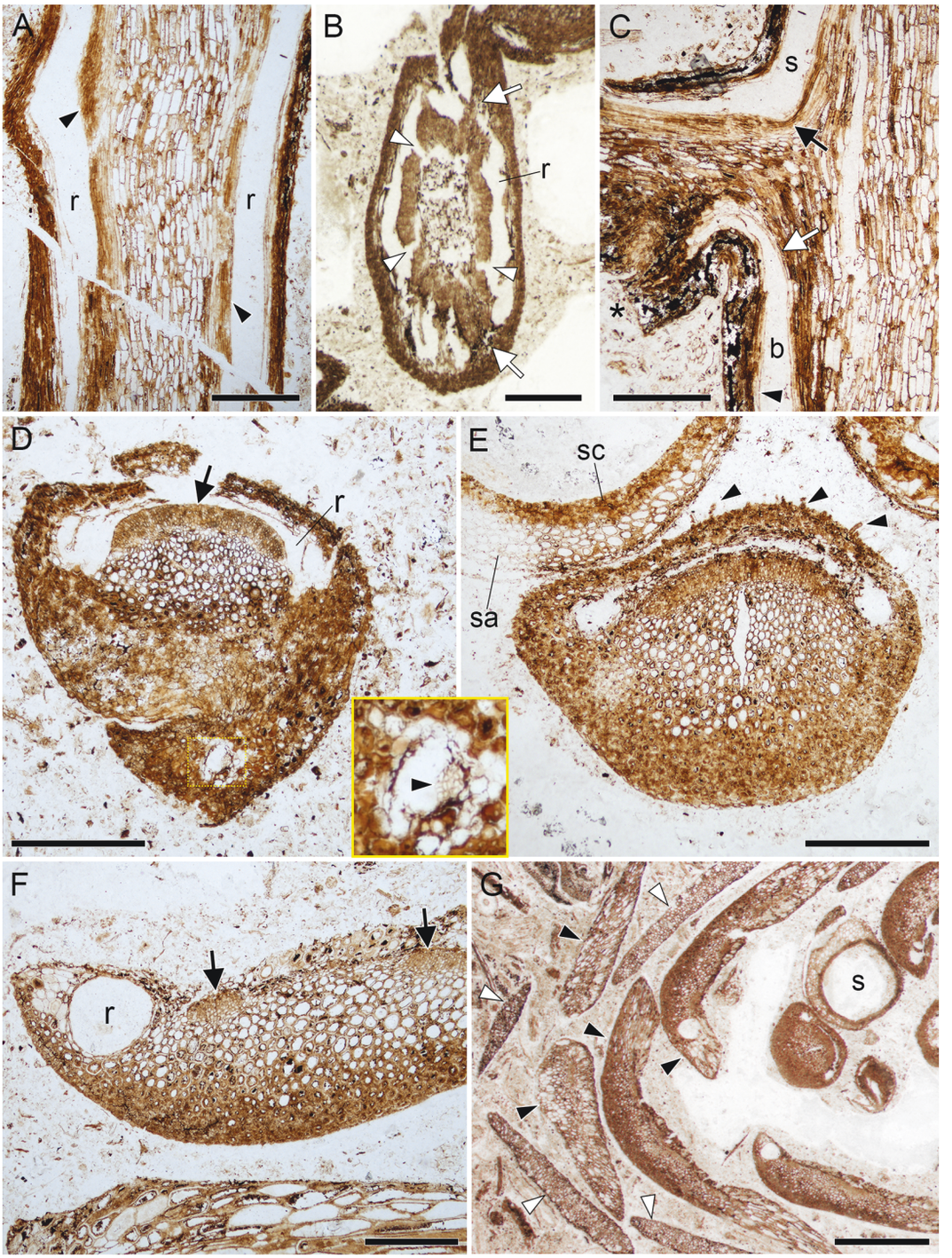

Fig. 3 Cone anatomy of *Schizolepidopsis ediae* sp. nov. from chert permineralizations. *A*, Longitudinal section through the cone axis from figure 1*D*, showing the sclerenchymatous outer cortex, wide resin cavity of the inner cortex (r), secondary xylem (arrowheads), and wide parenchymatous pith centrally. PB23507, peel 2. Scale bar = 500 μm. *B*, Oblique transverse section through a cone axis. The resin cavity (r) occupies the entire inner cortex, encircling the secondary xylem, and is disrupted only where vascular traces depart into bract-scale complexes (arrows). Note that the secondary xylem forms a continuous ring around the pith that is torn in several places (arrowheads). PB23506A, peel 0. Scale bar = 1 mm. *C*, Detail of the bract-scale complex's divergence from the cone axis in longitudinal section. Note that the resin canals supplying the bract (b) and ovuliferous scale (s) have separate origins from within the cone axis. Vascular traces supplying the bract and scale are indicated by white (bract) and black (scale) arrows. Note the epithelial cells lining the resin cavity (e.g., arrowhead) and that the bract is broken off at the base (asterisk). PB23507, peel 2. Scale bar = 500 μm. *D*, Slightly oblique transverse section through the fused bases of the bract (*bottom*) and ovuliferous scale (*top*). The ovuliferous scale has a large dumbbell-shaped resin canal (r) that curves over the wide vascular bundle (arrow). Note that the ovuliferous scale is mostly composed of thick-walled sclerenchyma, except for a zone of large thinner-walled cells abaxial to the vascular bundle. The bract is also sclerenchymatous, with a central resin canal abutting a small vascular bundle composed of primary xylem (arrowhead, *inset*). PB23508, peel 1. Scale bar = 500 μm. *E*, Transverse section through an ovuliferous scale base distal to that in *D*, showing a dumbbell-shaped resin canal and

Locality. Tevshiin Govi coal mine, central Mongolia. Zhahanaoer locality, Inner Mongolia, China.

Stratigraphic position and age. Tevshiin Govi Formation, probable Aptian-Albian stage, Early Cretaceous (Ichinnorov 2003, 2005). Huolinhe Formation, Early Cretaceous (Xu et al. 2013).

Etymology. The specific epithet *ediae* honors Dr. Edith L. Taylor for her numerous contributions to paleobotany and our understanding of seed plant evolution and for her advocacy for women in science.

Description

Cone morphology. Cones are slender, elongate, and cylindrical, measuring 7.0–12.0 mm wide and at least 3.5 cm long (fig. 1*A*, 1*B*). No complete cones have been recovered, so the full length is not known. The cones are compact, with imbricate, helically arranged bract-scale complexes (fig. 1*A*, 1*B*). The bract and ovuliferous scale are fused at the base for approximately 0.5–1.5 mm (fig. 1*C*, 1*D*). The fused bases of the bract-scale complexes form a stalk and diverge from the cone axis at right angles before curving apically (fig. 1*D*–1*F*). Distal to this point of curvature, the bract and the ovuliferous scale are free and the scale is laminar (fig. 1*C*, 1*D*). The laminar region of the ovuliferous scale is deeply bilobed, with the scale lobes diverging near the distal end of the seed body (figs. 1*A*–1*C*, 2). The laminar portion of the scale is 4.0–8.0 mm long (measured from the base to the apex of one lobe), with the free portions of the lobes one to two times longer than wide. Scale lobes are widest near the middle (2.0–3.0 mm wide) and taper slightly toward their apexes (fig. 2), which vary from short-acuminate to rounded, sometimes within the same cone (fig. 1*A*).

The bract is linear with a short-acuminate apex and twice as long or more than the ovuliferous scale it subtends (fig. 1*C*). Intact bracts are rarely preserved and are found only in lignite specimens with exceptional preservation (PP59844). Such specimens appear to be in a developmental stage near maturity but before dispersal, based on the presence of seeds in the cones. The only completely intact bract recovered is 11 mm long and approximately 0.5 mm wide (fig. 1C, white arrowhead). In most lignite specimens, bracts are represented by a scar or broken base approximately 1.0–1.5 mm below the cleft between the two lobes of the ovuliferous scale (fig. 2*E*, arrowhead). Intact bracts were not preserved in any of the permineralized cones (fig. 1*B*, 1*D*–1*F*). No evidence of a bract abscission zone was observed in these specimens, but bracts are consistently detached at the very base, where they separate from the ovuliferous scale, even in cones with seeds (figs. 1*F*, 3*C*). In such specimens, the dense packing of cone elements means that the bases of the bracts would have been protected from abrasion for several millimeters. Moreover, bract bases are heavily sclerified (fig. 3*D*), which could obscure abscission tissues. These features, particularly the consistent absence of bracts or irregular bract bases, indicate that the bracts were probably deciduous. Bracts were perhaps shed before seed maturation and dispersal since bracts were observed only in specimens with seeds and all specimens without seeds lacked intact bracts. Given the length of the bracts, it is possible that bracts were abscised to avoid obstructing dispersal of the winged seeds.

Cone anatomy. The cone axes are slender, ~3.0 mm wide, with a pith containing large elongate, rectangular cells 115–170 μm long and 23–48 μm wide (fig. 3*A*). Many of these cells are thin walled and parenchymatous but are interspersed among cells with thicker walls (fig. 3*A*). The pith is surrounded by a ring of vascular tissues mostly comprising secondary xylem (fig. 3*B*). No tissues that could be clearly identified as phloem were observed in the permineralized specimens. To the outside of the vascular tissues is a resin cavity 160–270 μm wide that spans the entire circumference of the cortex, although it is discontinuous in most transverse sections owing to gaps left by the departure of the resin cavity into bract-scale complexes (fig. 3*A*, 3*B*). In longitudinal section, the cortical resin cavity appears to be bordered by elongate, thin-walled epithelial cells (fig. 3*C*). The outmost layer of cortex consists of three or four layers of darkly colored narrow cells with thick, lignified secondary walls (fig. 3*A*–3*C*).

Basal regions of the ovuliferous scale are composed primarily of dark, thick-walled sclerenchyma (fig. 3*D*, 3*E*). Zones comprising larger cells with thinner walls occur centrally, abaxial to the vascular trace in the base of the scale, and adaxially, in the laminar region of the scale (fig. 3*E*, 3*F*). Distal regions of the scale lobes are mostly parenchymatous (fig. 3*G*). Similarly, bract bases are composed almost entirely of dark, thick-walled sclerenchyma (fig. 3*D*). The epidermal cells are small, with narrow lumina, while those of the ground tissue are larger, with variable secondary wall thickness (fig. 3*D*).

Vascular traces to the bract and ovuliferous scale originate as separate strands from within the cone axis, rather than as a single trace that branches to supply the bract and scale (fig. 3*C*; Miller 1976). The ovuliferous scale is supplied by a single large abaxially concave vascular trace, approximately 680 μm wide, that consists mostly of secondary xylem (fig. 3*D*, 3*E*). Within the scale, the trace branches once, proximal to the divergence of the two scale lobes (fig. 3*F*), and often branches again in each scale lobe. The bract is supplied by a single small vascular trace composed of primary xylem (fig. 3*D*). In the bract base, this trace is adjacent to and abuts the single large resin canals (fig. 3*D*). Whether this trace branches within the bract is unknown since intact bracts are not present in the permineralized specimens studied here.

The resin canals supplying the bract and scale also have separate origins in the cone axis (fig. 3*C*). The base of the ovuliferous scale contains a broad resin canal shaped like a curved dumbbell that surrounds the adaxial side of the vascular bundle (fig. 3*D*, 3*E*). This resin canal branches distally within the scale to form two round canals, each of which extends along the lateral edges of the scale (fig. 3*F*). They do not appear to extend into the scale

an abaxially concave vascular bundle. Note that there are no traces of the subtending bract, which has broken off. The adaxial surface of the scale base has several trichomes and trichome bases (arrowheads; see fig. 4*H* for detail). The structures adaxial to the scale base are seeds. Note the oblique section through the sclerotesta (sc) and thinner-walled cells of the sarcotesta (sa). PB23506, peel 2. Scale bar = 500 μm. *F*, Oblique transverse section through the laminar region of an ovuliferous scale, proximal to where the scale lobes diverge, showing a circular resin canal (r) on the lateral edge. Note the histological differences between the adaxial (*top*) and abaxial (*bottom*) sides of the scale and the two vascular bundles (arrows). PB23506A, peel 2. Scale bar = 200 μm. *G*, Oblique longitudinal section through a cone, showing transverse sections through the ovuliferous scales at different levels. Distally, the ovuliferous scale lobes are composed of small relatively uniform thin-walled cells (white arrowheads), whereas proximally, cell size and shape are more heterogeneous (black arrowheads). Note the seed (s) in transverse section. PB23506A, peel 0. Scale bar = 2 mm.

lobes. The bract contains a single central resin canal at the base, 95 μm in diameter at the widest point (fig. 3*D*).

Seeds. The seed body is asymmetric and roughly ovoid, 2.0–4.0 mm long (figs. 2*B*–2*F*, 4*A*–4*C*). Most cone specimens lack seeds, which were probably shed before fossilization. Seeds are typically two per ovuliferous scale (fig. 4*D*). In one specimen, some scales have a single large seed positioned in the center of the scale, possibly as a result of the abortion of the other ovule or seed. Ovuliferous scales have basal adaxial indentations corresponding to the positions of the seed bodies (figs. 2*A*, 2*B*, 4*D*). Seeds are composed of a thin poorly preserved sclerotesta surrounded by a parenchymatous sarcotesta with thickened primary walls (fig. 3*E*). Megagametophytes or embryos are not preserved, but μCT scans of one specimen (PB23509) show differentiated zones within the seed that could represent megagametophye, embryo, or nucellar tissues (fig. 4*G*).

Lignitized specimens reveal that seeds have a single distal wing derived from the entire adaxial surface of the scale (fig. 2*C*–2*F*). In the lignite, the cone scales that lack seeds have thinner, more ragged apexes, and the adaxial surface is dull rather than a lustrous gray. The dull and ragged appearance of the cone scales, as compared with those with intact seeds, probably results from the loss of the cuticle when the seed wing was shed. Two permineralized cones contained seeds (figs. 1*F*, 2*B*, 3*E*, 4*D*–4*G*), but neither shows clear evidence of wings in distal sections of ovuliferous scales (fig. 3*G*). This could be related to the developmental stages at which these cones were preserved, at which time the seed wing might not have differentiated or become detached from scale tissues. However, one specimen shows that the distal portion of the seed forms a continuous layer with the adaxial surface of the cone scale (fig. 4*F*), which likely forms the wing later in development.

Micropyles, which are oriented toward the cone axis, are well preserved in one permineralized specimen (PB23509; fig. 4*A*–4*G*). Seeds are oriented obliquely relative to the longitudinal axis of the ovuliferous scale (fig. 2*B*–2*F*), such that the micropyles project beyond the edges of the scale on either side of the scale base and are curved downward, toward the base of the cone (fig. 2*B*). Deeply lobed micropyles forming two micropylar arms similar to those of extant Pinaceae (fig. 4*B*, 4*C*) are revealed in μCT scans. The micropylar arms and the seed body are covered densely in trichomes (fig. 4*G*, 4*H*). Trichomes are also present on the cone axis, as well as on the base of the ovuliferous scale, proximal to the seeds (fig. 3*E*). The trichomes are uniseriate and multicellular, comprising at least two cells (fig. 4*H*). In lignitized cones, micropyles are preserved as a thin protruding beak on the seeds (fig. 2*D*, 2*E*), but micropylar arms and trichomes were not observed. Their absence in these specimens could be due to loss during preservation or development since these features are unlikely to persist into later developmental stages (Owens et al. 1998). Additionally, preserved trichomes could have been abraded during preparation of the fossils.

Phylogenetic Analyses

Results of the phylogenetic analyses are summarized in figures 5–7. For the *S. ediae*–only analyses (in which *S. ediae* was the only fossil taxon), *S. ediae* was consistently placed with high support in Pinaceae (posterior probability [PP] = 1.0, bootstrap support [BS] = 99), within the abietoid clade (PP = 0.95, BS = 64), and allied with *Tsuga canadensis* L. and *Nothotsuga longibracteata* (W.C.Cheng) H.H.Hu ex C.N.Page (PP = 0.94, BS = 59; figs. 5–7). The parsimony analyses yielded three MPTs, all of which placed *S. ediae* in a clade with *Tsuga* and *Nothotsuga*. In the parsimony bootstrap analysis, *S. ediae* was placed on the Pinaceae stem in a subset of replicates, indicating that relatively few characters support affinities with *Tsuga* and *Nothotsuga*. Four characters support this clade: 47, mode of seed release (cone spreading), 58, secondary xylem of cone axis (continuous cylinder), 64, resin canals at scale base: abaxial to trace (absent), and 67, bract resin canal number (one). Characters 64 and 67 represent unambiguous transitions, whereas 47 and 58 are ambiguous reversals to these character states within the abietoid clade. Trees in which *S. ediae* is placed in the crown group are shorter (tree length, 117 for the abietoid clade and 118 for the pinoid clade vs. 119 for the stem group) and have higher likelihood scores, but these likelihoods are not statistically different from one another on the basis of one-tailed Shimodaira-Hasegawa tests (see app. D). Nevertheless, crown placement of *S. ediae* within the abietoid clade was favored by Bayesian and parsimony analyses.

For the data set including all fossil species, the parsimony backbone analysis yielded 84 MPTs (tree length, 164). The 50% majority-rule consensus tree places *S. ediae* in the Pinaceae crown group (MPTs = 83%), in the abietoid clade with *Tsuga* and *Nothotsuga* (MPTs = 57%; fig. 6), and with the other three *Schizolepidopsis* species, forming a grade of successive sister taxa to crown Pinaceae. All MPTs place *S. ediae* either in the crown group with *Tsuga* and *Nothotsuga* or in various positions on the stem. Similar to the results of the *S. ediae*–only analyses, trees with *S. ediae* in the crown have higher likelihoods, but these likelihoods are not statistically different from those in which *S. ediae* is positioned on the stem (see app. D). The Bayesian majority-rule consensus topology is nearly identical to that of the parsimony consensus tree with respect to *S. ediae*, which forms a clade with *Tsuga* and *Nothotsuga* (PP = 0.62) within the Pinaceae crown group (PP = 0.87).

Eathiestrobus mackenziei is placed in the pinoid clade in parsimony (MPTs = 100%) and Bayesian consensus trees (PP = 0.63; fig. 7). These results are consistent with previous analyses that placed *E. mackenziei* either with pinoids or on the Pinaceae stem (Smith et al. 2016; Gernandt et al. 2018). In both Bayesian and parsimony analyses, *Cordaixylon dumusum*, *Emporia lockardii*, and *Hanskerpia hamiltonensis* were placed outside crown conifers. In the Bayesian analysis, *C. dumusum*, *E. lockardii*, and *H. hamiltonensis* formed a clade (PP = 0.77; fig. 6), whereas in the parsimony analysis, they were placed as successive sister taxa to crown conifers along with *Telemachus aequatus* and *Voltzia hexagona*. In the Bayesian analysis, *V. hexagona* was positioned in a polytomy outside crown conifers, and *T. aequatus* was sister to *Sciadopitys verticillata* (PP = 0.66; fig. 6). *Pararaucaria patagonica* was placed as sister to Podocarpaceae (PP = 0.63) in the Bayesian analysis and sister to Podocarpaceae plus Araucariaceae in the parsimony consensus tree (MPTs = 79%; fig. 7).

Discussion

Conspecificity of Lignite and Chert Specimens and Comparison with Other Species

We consider cones preserved in lignite at the Tevshiin Govi mine in Mongolia and those preserved in chert at the Zhahanaoer locality in Inner Mongolia, China, as the same species, established here as *Schizolepidopsis ediae*. Despite preservational differences

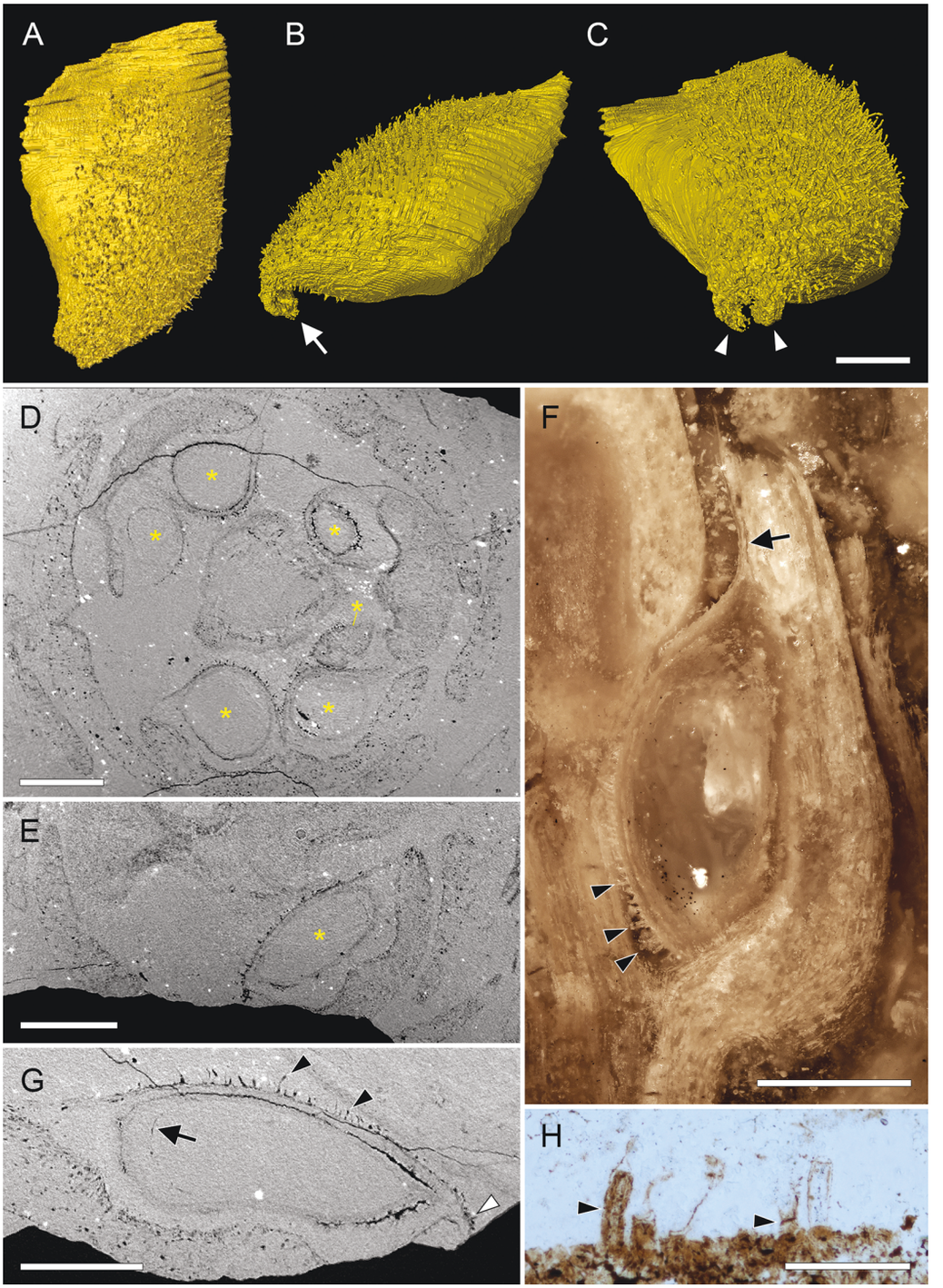

Fig. 4 Seeds of *Schizolepidopsis ediae* sp. nov. from chert permineralizations. *A–C*, Three-dimensional reconstruction of a seed body from a micro–computed tomography (μCT) scan. Seeds are covered densely in trichomes adaxially, as well as on the micropyle (arrow). Note the two curved micropylar arms (arrowheads). PB23509, holotype. Scale bar = 1 mm. *D*, *E*, Transverse sections through a cone with seeds from a μCT scan. Most ovuliferous scales bear two seeds (asterisks), as seen in *D*, but some have a single larger seed that occupies the entire scale (*E*). Note the indentations in the adaxial surface of the ovuliferous scales corresponding to seeds in *D* and their presence in *E* despite the development of only one seed. PB23509, holotype. Scale bars = 1 mm. *F*, Longitudinal section through a seed and ovuliferous scale as seen on the fractured surface of the chert. The seed body forms a continuous tissue layer with the adaxial surface of the scale at the distal end, which likely develops into the seed wing (arrow). Note the trichomes on the seed (arrowheads). PB23509, holotype. Scale bar = 1 mm. *G*, Longitudinal section through a seed from a μCT scan in which two distinct tissue layers are visible within the seed. The arrow indicates the line delineating them at the chalazal end. Note the micropyle (white arrowhead) and trichomes (black arrowheads). PB23509, holotype. Scale bar = 1 mm. *H*, Detail of trichomes on the ovuliferous scale base from figure 3*E*. The trichomes are uniseriate and multicellular. The arrowheads indicate walls separating adjacent cells. PB23506A, peel 2. Scale bar = 100 μm.

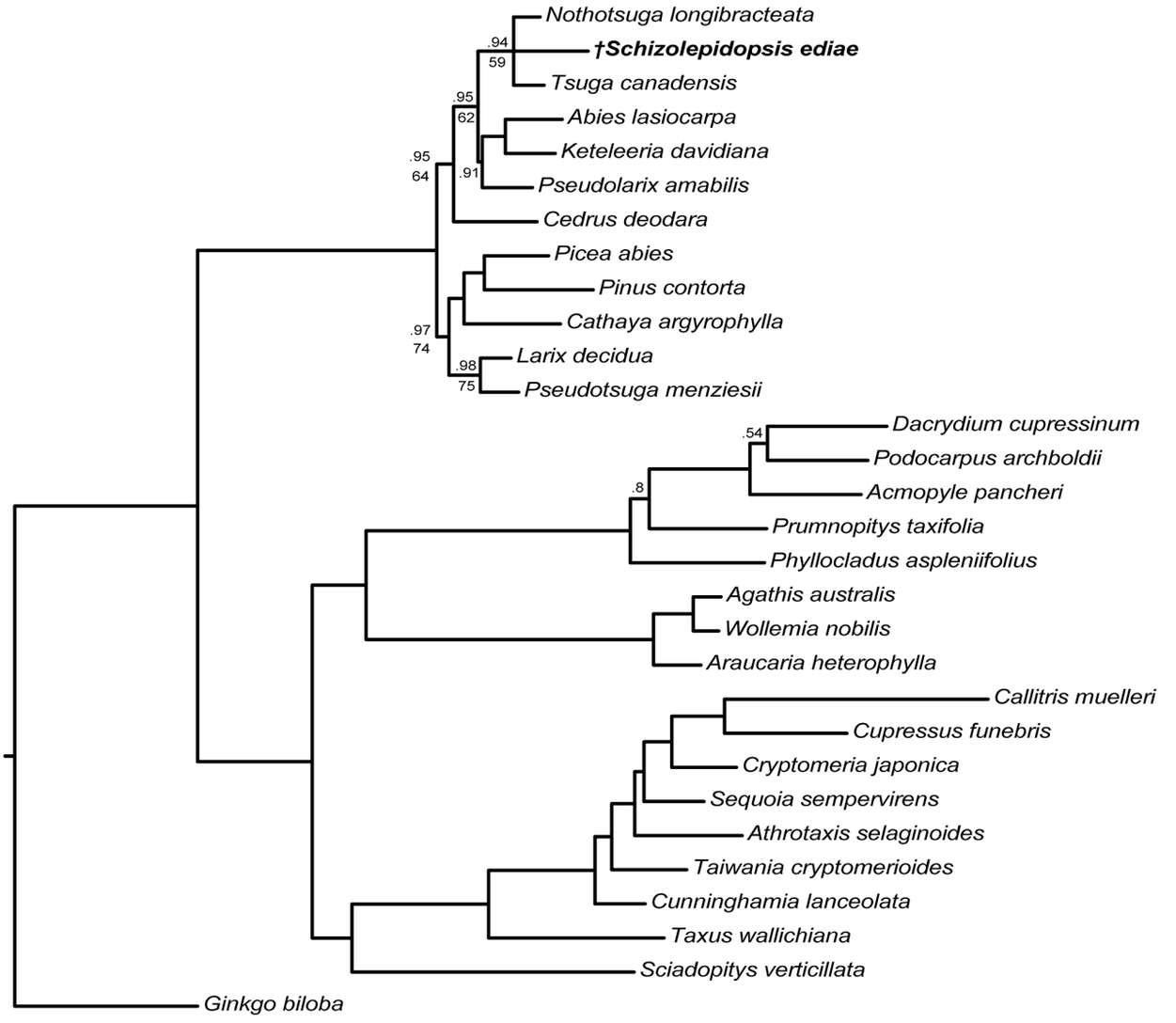

Fig. 5 Phylogenetic relationships of *Schizolepidopsis ediae* sp. nov. based on Bayesian total evidence and parsimony backbone analyses. The fossil taxon is indicated with a dagger and bold tip label. Branch lengths from the Bayesian analysis are shown. Support values indicate posterior probabilities (*top*) and bootstrap values (*bottom*). Only support values below 0.99 and 99% are shown.

and the geographic distance between localities, the cones are morphologically identical to one another and distinct from previously described species of *Schizolepidopsis*, including *S. canicularis* from Tevshiin Govi (Leslie et al. 2013). We note that the specimen interpreted to be an immature cone of *S. canicularis* by Leslie et al. (2013; fig. 2*D*; PP55454) is a mature cone of *S. ediae*. Cones of *S. ediae* from both localities overlap in size and cone scale shape, and we documented no characters that distinguish them that are not also related to mode of preservation and taphonomy. For instance, micropylar arms and trichomes were not observed in lignite material, but their absence may reflect taphonomic or developmental factors.

Schizolepidopsis comprises at least 79 currently recognized species spanning the late Permian through the Early Cretaceous, with the earliest records from the late Permian being the most uncertain (Domogatskaya and Herman 2019). Many of these species, particularly the oldest occurrences, are poorly understood. Some are described from incompletely preserved compression fossils, consist of isolated bract-scale complexes, or lack informative illustrations, making specimens difficult to evaluate without examining original material. Thus, exhaustive comparisons with all previously described species are beyond the scope of this study. Instead, we summarize some of the uniting characters of *Schizolepidopsis*, the variation documented among species, and characters that distinguish *S. ediae* from others.

All *Schizolepidopsis* are united by having bilobed ovuliferous scales and two seeds per scale, but there is considerable variation in the morphology of the cones and bract-scale complexes. Many cones are lax in structure, with long internodes, while others are more compact, with imbricated scales (Zhang et al. 2011). In some species, the lobes are deeply divided and are united below the laminar region of the scale and the point of seed attachment (Zhang

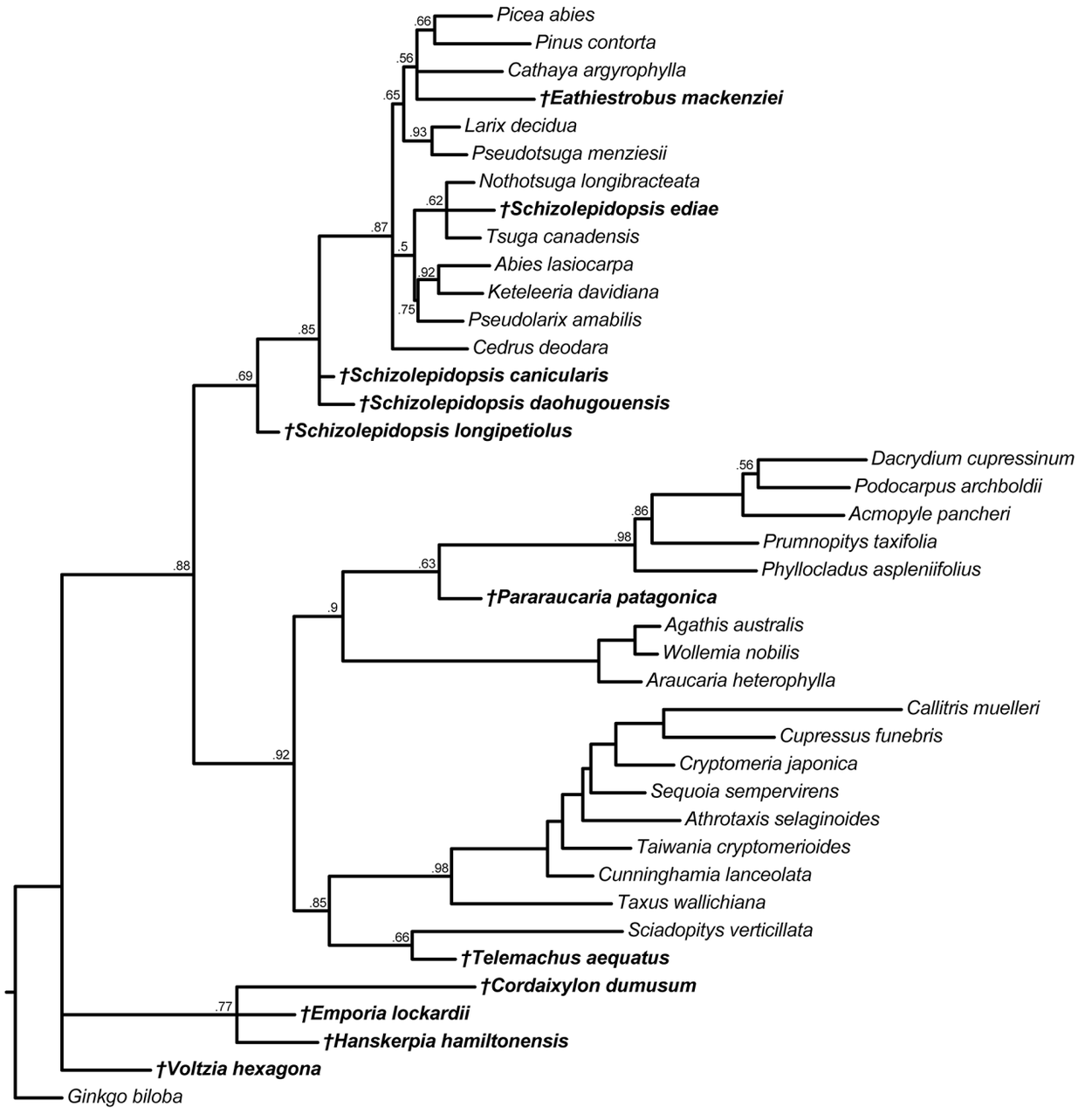

Fig. 6 Phylogenetic relationships of *Schizolepidopsis ediae* sp. nov. and nine fossil conifers from a Bayesian total evidence analysis. Fossil taxa are indicated with a dagger and bold tip labels. Node labels represent posterior probabilities. Only values below 0.99 are shown.

et al. 2011; Leslie et al. 2013). In others, the lobes are divided for approximately one-half to two-thirds the length of the scale and are united at the level of the seed body (Zhang et al. 2011), as is the case for *S. ediae*. Ovuliferous scale lobes range from highly elongated to short and stout, with rounded to short-acuminate apexes.

Seed wings have been documented in only a few species of *Schizolepidopsis* (e.g., Doludenko and Kostina 1985; Doludenko et al. 1995; Zhang et al. 2011; Leslie et al. 2013), and their absence has made placement of the genus within Pinaceae equivocal (Zhang et al. 2011; Rothwell et al. 2012; Leslie et al. 2013). While it is possible that the trait is variable within the genus, with some species having no wing or small underdeveloped wings (e.g., similar to some extant *Pinus*), many *Schizolepidopsis* species are poorly or incompletely preserved, and thus the absence of wings could reflect preservational factors. When seed wings are present, they appear to be derived from the entire adaxial surface of the ovuliferous scale and might therefore be especially difficult to identify in compression fossils.

Bracts are rarely observed but are usually described as short or fan shaped (Zhang et al. 2011). Most often, the presence of the bract is indicated only by a scar at the base of the scale. Long

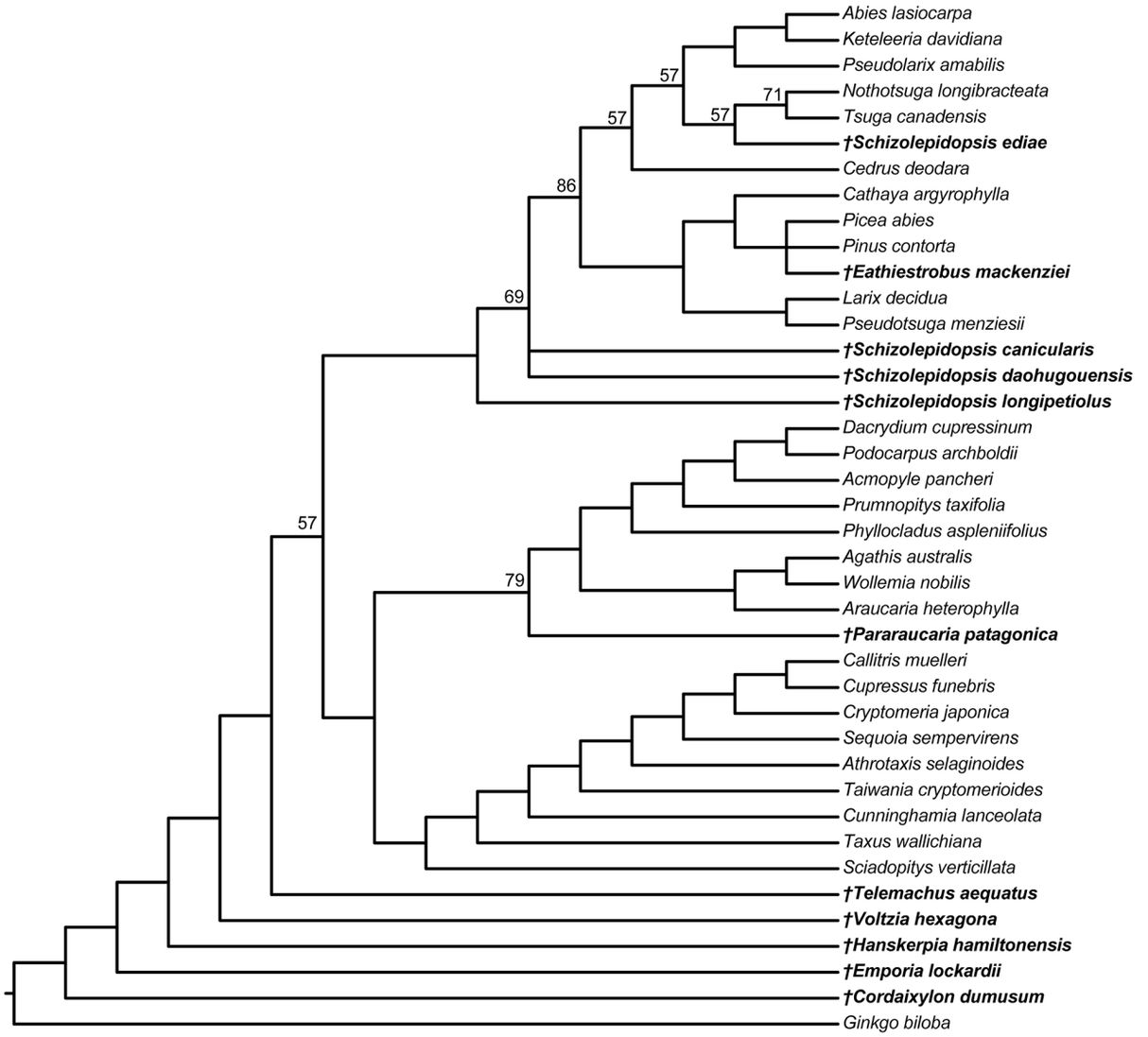

Fig. 7 Majority-rule consensus tree of 84 most parsimonious trees (MPTs) from a parsimony backbone analysis of *Schizolepidopsis ediae* sp. nov. and nine fossil conifers. Node labels indicate the percentage of MPTs that support a clade. Only values below 100% are shown. Fossil taxa are indicated with a dagger and bold tip labels. Note the differences in the placement of *Telemachus aequatus* and *Pararaucaria patagonica* in this analysis compared with the Bayesian total evidence analysis in figure 6.

linear bracts like those of *S. ediae* have not been documented in *Schizolepidopsis* previously. It is notable that a few species have been described as having trilobed rather than bilobed cone scales (Zhang et al. 2011). In *S. trilobata*, the central lobe is linear and both longer and narrower than the other two lobes (Wang et al. 1997). Domogatskaya and Herman (2019) considered the trilobed morphology to be an aberrant form, but an alternative interpretation could be that the central lobe is a linear bract similar to that of *S. ediae*.

At Tevshiin Govi, *S. canicularis* was described from seed cones and isolated bract-scale complexes. Overall, cones of *S. canicularis* are more lax than those of *S. ediae* and much larger, measuring up to 2.7 cm wide with ovuliferous scales up to 27 mm long, compared with cones up to 12 mm wide and scales up to 8 mm long in *S. ediae*. The free portions of the ovuliferous scale lobes are more elongated than those of *S. ediae*, and the lobes diverge proximal to the point of seed attachment rather than distally, as in *S. ediae*. Bract scars of *S. canicularis* show a central vascular strand and two lateral resin canals, in contrast to the single central resin canal and vascular strand in *S. ediae*. Seeds of *S. canicularis* are winged, like those of *S. ediae*.

Two species have been described from other localities in the Huolinhe Formation, from which the chert specimens also originate: *S. longipetiolus* (Xu et al. 2013) and *S. moelleri* Seward (Wang et al. 1997). Both species were described from compression fossils. Cones of *S. longipetiolus* are lax, with relatively long internodes separating bract-scale complexes. Ovuliferous scales have a long stalk up to 7 mm long, and the scale lobes are up to

18 mm long, longer than those of *S. ediae*. There are also differences in the shape of the ovuliferous scale. In *S. longipetiolus*, the lobes are widest near the base, whereas in *S. ediae*, the lobes are widest in the middle. Additionally, in *S. longipetiolus*, unlike in *S. ediae*, the two scale lobes diverge proximal to the point of seed attachment, and the seeds were described as lacking wings.

Schizolepidopsis moelleri was described from a single isolated bract-scale complex (Wang et al. 1997). Ovuliferous scale lobes are 11 mm long, widest near the base, and subtended by a structure interpreted as a bilobed bract. Seeds were not documented for this specimen.

Overall, the morphology of *S. ediae* fits within the range of variation documented for *Schizolepidopsis*. The salient characters that distinguish it from other species include the morphology of the bracts and the anatomical characters of the cones since no other *Schizolepidopsis* species have been described from permineralized specimens. In addition, *S. ediae* can be distinguished from other species of *Schizolepidopsis* described previously from Tevshiin Govi and the Huolinhe Formation on the basis of cone structure, cone size, the point of divergence of ovuliferous scale lobes, lobe shape, and, in the case of *S. longipetiolus*, the presence of a seed wing. These differences and the unprecedented anatomical preservation, which makes it difficult to compare many key characters with those of previously described species, support treatment of *S. ediae* as a new species within the genus.

The discovery of a new species of *Schizolepidopsis* at Tevshiin Govi adds to the diversity of the conifer assemblage at this locality. To date, six other conifer species have been described from Tevshiin Govi, as follows: the voltzialean *Krassilovia mongolica* Herrera, Leslie, Shi, Knopf, Ichinnorov, Takahashi, Crane et Herendeen; two species of Cupressaceae, *Pentakonos diminutus* Herrera, Shi, Knopf, Leslie, Ichinnorov, Takahashi, Crane et Herendeen and *Stutzeliastrobus foliatus* Herrera, Shi, Knopf, Leslie, Ichinnorov, Takahashi, Crane et Herendeen; and three pinaceous conifers, *S. canicularis*, *Picea farjonii* Herrera, Leslie, Shi, Knopf, Ichinnorov, Takahashi, Crane et Herendeen, and *Pityostrobus stockeyae* Herrera, Leslie, Shi, Knopf, Ichinnorov, Takahashi, Crane et Herendeen (Leslie et al. 2013; Herrera et al. 2015, 2016, 2017, 2020). In addition, two or more species of *Schizolepidopsis* cooccur at Tevshiin Govi in Mongolia (*S. ediae* and *S. canicularis*) and in the Huolinhe Formation of Inner Mongolia, China (*S. ediae*, *S. longipetiolus*, and *S. moelleri*), highlighting the diversity of the genus during the Late Cretaceous of East Asia (Domogatskaya and Herman 2019).

Functional Morphology and Pollination of S. ediae *Ovulate Cones*

Schizolepidopsis ediae produced elongate, compact cones with slender axes and bract-scale complexes borne on narrow stalks. Seeds were dispersed by cone spreading rather than by abscission of the ovuliferous scales. The long linear bracts were probably deciduous and shed before seed dispersal. These interpretations are supported by the frequent recovery of intact cones lacking both seeds and bracts, by the rare occurrence of intact bracts, and by the consistent truncation of the bracts at the very base. The structure and orientation of the micropyle, as well as the presence of trichomes on the seed and scale base, indicate that like modern Pinaceae, *S. ediae* probably produced a pollination drop and cones were upright at pollination. In living Pinaceae, such trichomes function as surfaces on which moisture beads, carrying pollen that has settled on the cone surface toward the micropyle (Owens et al. 1998). The micropyles point downward so that pollen cannot fall into the micropyle and must enter via the pollination drop. The pollination drop fills the space between the micropylar arms, and saccate pollen grains then float upward, into the micropyle toward the nucellus (Owens et al. 1998; Leslie 2010). The morphology of *S. ediae* suggests a similar pollination mechanism; the probable downward orientation of its micropyles would have prevented pollen from entering passively, and thus a pollination drop would have been necessary to achieve pollination. Although it is possible that the cones of *S. ediae* were not erect at pollination and thus the micropyles did not point downward, all of the morphological characters of the ovules (particularly the presence of micropylar arms) are consistent with a pollination mechanism like that of extant Pinaceae. We further speculate that the pollen of *S. ediae* was most likely saccate based on characters that are consistent with a downward-oriented pollination drop. Intriguingly, bisaccate pollen grains were observed in the micropyle of a seed of *S. canicularis* from Tevshiin Govi, suggesting that at least some species of *Schizolepidopsis* might have produced bisaccate pollen (Leslie et al. 2013).

Phylogenetic Relationships of Schizolepidopsis

Phylogenetic analyses based on ovulate cone characters provide strong support for a close relationship between *S. ediae* and extant Pinaceae. This is consistent with the presence of several key characters of living Pinaceae, including compact cones with two seeds per ovuliferous scale, seed wings derived from ovuliferous scale tissue, a well-developed bract subtending and mostly free from the ovuliferous scale, the presence of micropylar arms, and the separate origins of vasculature and resin canals supplying bracts and ovuliferous scales (Miller 1976; Owens et al. 1998; Gernandt et al. 2018). Among living conifers, seed wings derived from scale tissue are unique to Pinaceae, as are well-differentiated bracts and scales that are fused only at the base. However, well-differentiated and unfused or partially fused bract-scale complexes are also found among extinct voltzialeans (Clement-Westerhof 1988). One notable difference between *S. ediae* and Pinaceae, both fossil and extant, is the architecture of the resin system within the cone. In *S. ediae*, the cone axis possesses a large cortical resin cavity that extends into the bracts and scales as resin canals. By contrast, most Pinaceae cones have discrete resin canals within the axis.

Placement of *S. ediae* in the Pinaceae stem versus the crown group appears to be sensitive to the inclusion of other fossils, particularly other species of *Schizolepidopsis*. Support for the Pinaceae crown node is consistently high when *S. ediae* is included, indicating that *S. ediae* can be confidently considered part of the Pinaceae total group (crown and stem group). However, its placement relative to living members of Pinaceae is less certain. When *S. ediae* is the only fossil included in the analysis, placement within the crown group as part of the abietoid clade (allied with *Tsuga* and *Nothotsuga*) is well supported in the Bayesian analysis but receives moderate support in parsimony analyses since *S. ediae* is placed on the Pinaceae stem in a subset of parsimony bootstrap samples. The low bootstrap values, as compared with PPs for the same nodes, reflect sensitivity to character resampling for placement within the Pinaceae crown group, which is consistent with

there being few unambiguous character changes that support crown placement of *S. ediae*. However, trees in which *S. ediae* is placed on the stem are longer in terms of character changes than those in which *S. ediae* is placed in the crown.

When other fossil conifers are included in the analyses, the placement of *S. ediae* becomes more uncertain. The Bayesian and parsimony consensus trees still place *S. ediae* with *Tsuga* and *Nothotsuga* but with lower support (fig. 6). Most parsimonious topologies that place *S. ediae* in the crown group rather than on the stem tend to have higher likelihood scores, but these differences in likelihoods are not statistically significant (see app. D). Interestingly, these uncertainties are primarily driven by the inclusion of other species of *Schizolepidopsis*. Analyses that included other fossil conifers but with *S. ediae* as the only species of *Schizolepidopsis* yielded results similar to those of the *S. ediae*–only analyses (see app. D). Taken together, while the phylogenetic analyses overall favor the placement of *S. ediae* in the Pinaceae crown group, stem group affinities are still possible, and the morphological characters used here do not provide overwhelming evidence in support of one topology over the other. This is perhaps unsurprising when considering the characters that unite *S. ediae* with *Tsuga* and *Nothotsuga* and the abietoid clade more generally. Affinities with *Tsuga* and *Nothotsuga* are supported by four characters, but only two of these represent unambiguous character state transitions. For the abietoid clade, the only unambiguous character state transition is the shift to stalked ovuliferous scales. However, the distribution of this character state is altered by the inclusion of the other *Schizolepidopsis* species, all of which have stalked scale bases; thus, when *Schizolepidopsis* is positioned along the Pinaceae stem, stalked ovuliferous scales are no longer a synapomorphy for the abietoid clade, weakening the relationship between *S. ediae* and the Pinaceae crown group. Therefore, a conservative interpretation of our results would be to consider *S. ediae* a late-diverging stem to early-diverging crown member of Pinaceae. We also stress that these results are based only on ovulate cones, and many anatomical characters could not be scored for the other *Schizolepidopsis* species, which are preserved as coalified or lignitized compressions. Other aspects of the morphology of *Schizolepidopsis* that might alter phylogenetic relationships are not known.

Phylogenetic placement of *Schizolepidopsis* with respect to the crown and stem group of Pinaceae has important implications for the age of the family because occurrences of *Schizolepidopsis* extend into the Triassic and possibly the Late Permian (Domogatskaya and Herman 2019). Crown group placement of the genus, as suggested by the *S. ediae*–only analyses, could therefore potentially push the origin of Pinaceae into the Paleozoic, a scenario that is incongruent with molecular and other fossil evidence. Analyses of the full fossil data set instead indicate that the genus *Schizolepidopsis* is not monophyletic and is a paraphyletic or possibly polyphyletic assemblage, at least some members of which are stem group Pinaceae. A nonmonophyletic *Schizolepidopsis* is consistent with some of the variability within the genus, most notably the apparent absence of seed wings in many species, and other voltzialean characters like lax cone structure and complex lobed ovuliferous scales. More importantly, recognition of *Schizolepidopsis* as a Pinaceae stem group has implications for understanding morphological evolution in Pinaceae because stem taxa can help to reveal character changes that occurred in the evolution of the crown group. The most conspicuous of these changes is the transition from bilobed to simple ovuliferous scales. Interestingly, the distinct bilobed morphology of *Schizolepidopsis* ovuliferous scales does not occur in wild-type individuals of living Pinaceae but is known from teratologies (Guédès and Dupuy 1971, 1974; Carlsbecker et al. 2013).

Evolutionary Development of Bilobed Ovuliferous Scales in Pinaceae

The ovulate cones of living conifers are widely regarded as compound, containing ovuliferous scales that are homologous with reduced ovule-bearing shoots borne in the axil of a bract (Gifford and Foster 1989). This hypothesis was popularized by the syntheses presented by Florin (1954), which detailed anatomical and developmental evidence for this morphological interpretation and proposed that ovuliferous scales evolved by the reduction of axillary ovuliferous shoots like those found in the ovulate cones of cordaitalean gymnosperms (Stewart and Rothwell 1993; Spencer et al. 2015; Leslie et al. 2018). Intermediates in this evolutionary transformation include flattened axillary shoots bearing partially fused vegetative leaves and sporophylls and multilobed ovuliferous scales, as seen in many Paleozoic and Mesozoic conifers, notably the Voltziales (Clement-Westerhof 1988; Stewart and Rothwell 1993; Axsmith et al. 1998; Taylor et al. 2009). One molecular mechanism that could conceivably explain the diversity of ovulate cones in the fossil record involves expansion in the expression of genes suppressing meristematic activity in axillary ovuliferous shoots over evolutionary time (Carlsbecker et al. 2013). Developmental genetics of seed cones of *Picea abies* var. *acrocona* (*acrocona* mutants) provide evidence of such a mechanism and identify candidate genes involved in this process (Carlsbecker et al. 2013).

The *acrocona* mutants are characterized by homeotic transformations of vegetative long shoots into ovulate cones. In the transition zone between vegetative needle leaves and bract-scale complexes of ovulate cones, vegetative leaves are broader and more bract-like and have multilobed ovule-bearing structures in their axils (Guédès and Dupuy 1974; Carlsbecker et al. 2013). These lobed axillary structures are typically bilobed or trilobed and strongly resemble the ovuliferous scales of *Schizolepidopsis* (including the rare reports of trilobed *Schizolepidopsis* cone scales). Gene expression patterns in the abnormal *acrocona* cone scales revealed normal expression of the MADS-box gene *DAL2* but dramatic reduction in the expression of *DAL14*, indicating that *DAL14* is normally involved in suppressing the formation of multilobed axillary structures (Carlsbecker et al. 2013). *DAL2* and *DAL14* are homologues of angiosperm genes involved in meristem determinacy and floral meristem identity (Carlsbecker et al. 2013), with *DAL2* also being orthologous to genes used as markers of ovuliferous scale identity in conifers (Englund et al. 2011). Similar genetic mechanisms involving changes in the gene expression patterns of *DAL2* and *DAL14* homologues could, therefore, have been involved in the evolutionary transformation of ovuliferous dwarf shoots, as proposed by Florin (Carlsbecker et al. 2013; Ruelens and Geuten 2013).

Although such a mechanism for the evolution of conifer ovuliferous scales remains speculative, the *acrocona* system nevertheless provides important information for understanding the morphology of *Schizolepidopsis*, the bilobed ovuliferous scales of which could have resulted from relatively small changes in patterns

of gene expression in developing ovulate cones. Similar bilobed cone scales have also been documented in *Pinus*, indicating that this teratology is not restricted to *Picea* (Guédès and Dupuy 1971). Importantly, these studies demonstrate that modern Pinaceae retain the molecular machinery to produce morphologies found in the fossil record and provide a plausible developmental link between the bilobed ovuliferous scales of *Schizolepidopsis* and the simple scales of living taxa.

Implications for the Evolution of Pinaceae

The phylogenetic hypotheses of fossil and living conifers presented here suggest several features of morphological evolution in Pinaceae. The first pertains to the evolution of seed wings derived from the ovuliferous scale, a trait that characterizes living Pinaceae. Both *S. canicularis* and *S. daohugouensis* have distal seed wings derived from the ovuliferous scale, whereas *S. longipetiolus* does not. All three species were placed as Pinaceae stem taxa, with *S. longipetiolus* usually attached at more basal nodes in the tree. This indicates that ovuliferous scale seed wings evolved along the Pinaceae stem and not with the origin of the crown group, in the most parsimonious scenario. This is important for understanding which traits of living Pinaceae truly characterize the crown group. The second pertains to the evolution of ovuliferous scales, which are hypothesized as highly reduced axillary ovuliferous shoots (Florin 1954). The occurrence of bilobed ovuliferous scales in *Schizolepidopsis* and in teratological seed cones of living Pinaceae indicates that bilobed ovuliferous scales are likely a plesiomorphic character state in Pinaceae. Bilobed ovuliferous scales occurred in the stem group and possibly persisted in some crown taxa (depending on the position of *S. ediae*) but are absent in living species. This, in combination with developmental genetic studies of *acrocona* mutants, which provide a genetic mechanism for this change, implies that simple ovuliferous scales in Pinaceae likely evolved directly from bilobed ovuliferous scales. If this is the case, *Schizolepidopsis* bridges a morphological gap between the multilobed ovuliferous scales of voltzialean conifers and the simple scales of living Pinaceae. The inclusion of *Schizolepidopsis* in future phylogenetic analyses could therefore help to inform evolutionary relationships between Pinaceae and the Paleozoic conifers from which the family arose.

Fossils assigned to *Schizolepidopsis* span the late Permian through the Early Cretaceous (Domogatskaya and Herman 2019) and include species that possess characters of crown Pinaceae (e.g., *S. ediae*), as well as those similar to many voltzialean conifers (e.g., lax cone structure, wingless seeds). Although many *Schizolepidopsis* species are poorly understood and should be reexamined, our results indicate that *Schizolepidopsis* is closely related to Pinaceae. This helps to reconcile the apparent Carboniferous divergence of Pinaceae from other conifers (Leslie et al. 2018) with the much later appearance of modern-looking fossils in the Late Jurassic–Early Cretaceous (Rothwell et al. 2012; Smith et al. 2016) and the paucity of clear stem taxa deeper in the fossil record (Taylor et al. 2009; Rothwell et al. 2012). Although only a few *Schizolepidopsis* species were included in our study, they provide compelling evidence that some *Schizolepidopsis* belong to a Mesozoic Pinaceae stem group that potentially extends as far back in time as the Permian. Resolving these questions on the nature of the Pinaceae stem group and relationships with voltzialean conifers will require careful reevaluation of older species of *Schizolepidopsis* and phylogenetic analyses that include denser sampling of the conifer fossil record. Our study nevertheless provides the first firm evidence for a relationship between *Schizolepidopsis* and Pinaceae, an important step forward in elucidating the enigmatic evolutionary history of the largest family of living conifers.

Acknowledgments

We are grateful to two anonymous reviewers whose insightful and constructive feedback significantly improved this contribution. We also thank Dr. Ashley Klymiuk from the Field Museum of Natural History for assistance with the curation and accessioning of specimens. This research was generously funded by the National Science Foundation (DEB-1748286), the Oak Spring Garden Foundation (to F. Herrera), the National Natural Science Foundation of China (41772014), and the Youth Innovation Promotion Association, CAS (2017359; to G. Shi). We also thank Dr. Selena Y. Smith for providing access to the μCT facilities. This study includes data produced in the CTEES facility at the University of Michigan, supported by the Department of Earth and Environmental Sciences and College of Literature, Science, and the Arts.

Literature Cited

Andruchow-Colombo A, IH Escapa, RJ Carpenter, RS Hill, A Iglesias, AM Abarzua, P Wilf 2019 Oldest record of the scale-leaved clade of Podocarpaceae, early Paleocene of Patagonia, Argentina. Alcheringa 43:127–145.

Axsmith BJ, TN Taylor, EL Taylor 1998 A new fossil conifer from the Triassic of North America: implications for models of ovulate cone scale evolution. Int J Plant Sci 159:358–366.

Blokhina N, MA Afonin 2007 Fossil wood *Cedrus penzhinaensis* sp. nov. (Pinaceae) from the Lower Cretaceous of north-western Kamchatka (Russia). Acta Palaeobot 47:379–389.

Bomfleur B, AL Decombeix, IH Escapa, AB Schwendemann, B Axsmith 2013 Whole-plant concept and environment reconstruction of a *Telemachus* conifer (Voltziales) from the Triassic of Antarctica. Int J Plant Sci 174:425–444.

Carlsbecker A, JF Sundström, M Englund, D Uddenberg, L Izquierdo, A Kvarnheden, F Vergara-Silva, P Engström 2013 Molecular control of normal and *acrocona* mutant seed cone development in Norway spruce (*Picea abies*) and the evolution of conifer ovule-bearing organs. New Phytol 200:261–275.

Carothers IE 1907 Development of ovule and female gametophyte in *Ginkgo biloba*. Bot Gaz 43:116–130.

Clement-Westerhof JA 1988 Morphology and phylogeny of Paleozoic conifers. Pages 298–337 *in* CB Beck, ed. Origin and evolution of gymnosperms. Columbia University Press, New York.

Delevoryas T, RC Hope 1973 Fertile coniferophyte remains from the Late Triassic Deep River Basin, North Carolina. Am J Bot 60:810–818.

Doludenko MP, AI Kiritchkova, EI Kostina 1995 On the Jurassic flora of the Lenger coal deposits (South Kazakhstan). Paleontol Zh 1:98–109.

Doludenko MP, EI Kostina 1985 *Schizolepis fanica*: the Mesozoic representative of the family Pinaceae. Bot Zh 70:464–471.
Domogatskaya KV, AB Herman 2019 New species of the genus *Schizolepidopsis* (conifers) from the Albian of the Russian high Arctic and geological history of the genus. Cretac Res 97:73–93.
Dong M, G Sun 2012 *Ginkgo huolinhensis* sp. nov. from the Lower Cretaceous of Huolinhe Coal Field, Inner Mongolia, China. Acta Geol Sin 86:11–19.
Dörken VM, H Nimsch 2015 Morpho-anatomical investigations of cones and pollen in *Cathaya argyrophylla* Chung & Kuang (Pinaceae, Coniferales) under systematical and evolutional aspects. Feddes Repert 125:25–38.
Dörken VM, PJ Rudall 2018 Understanding the cone scale in Cupressaceae: insights from seed-cone teratology in *Glyptostrobus pensilis*. PeerJ 2018:1–19.
Englund M, A Carlsbecker, P Engström, F Vergara-Silva 2011 Morphological "primary homology" and expression of AG-subfamily MADS-box genes in pines, podocarps, and yews. Evol Dev 13:171–181.
Erdenetsogt BO, I Lee, D Bat-Erdene, L Jargal 2009 Mongolian coal-bearing basins: geological settings, coal characteristics, distribution, and resources. Int J Coal Geol 80:87–104.
Escapa IH, SA Catalano 2013 Phylogenetic analysis of Araucariaceae: integrating molecules, morphology, and fossils. Int J Plant Sci 174: 1153–1170.
Escapa IH, R Cúneo, B Axsmith 2008 A new genus of the Cupressaceae (sensu lato) from the Jurassic of Patagonia: implications for conifer megasporangiate cone homologies. Rev Palaeobot Palynol 151:110–122.
Escapa IH, GW Rothwell, RA Stockey, NR Cúneo 2012 Seed cone anatomy of Cheirolepidiaceae (Coniferales): reinterpreting *Pararaucaria patagonica* Wieland. Am J Bot 99:1058–1068.
Farjon A 2005 A monograph of Cupressaceae and *Sciadopitys*. Royal Botanic Gardens, Kew, UK.
——— 2017 A handbook of the world's conifers. Brill, Leiden, Netherlands.
Farjon A, SO Garcia 2002 Towards the minimal conifer cone: ontogeny and trends in *Cupressus*, *Juniperus* and *Microbiota* (Cupressaceae s. str.). Bot Jahrb Syst Pflanzengesch Pflanzengeogr 124:129–147.
——— 2003 Cone and ovule development in *Cunninghamia* and *Taiwania* (Cupressaceae sensu lato) and its significance for conifer evolution. Am J Bot 90:8–16.
Florin R 1954 The female reproductive organs of conifers and taxads. Biol Rev 29:367–389.
Gernandt DS, C Reséndiz Arias, T Terrazas, X Aguirre Dugua, A Willyard 2018 Incorporating fossils into the Pinaceae tree of life. Am J Bot 105:1329–1344.
Gifford EM, AS Foster 1989 Morphology and evolution of vascular plants. Freeman, New York.
Graham SA, MS Hendrix, CL Johnson, D Badamgarav, G Badarch, J Amory, M Porter, R Barsbold, LE Webb, BR Hacker 2001 Sedimentary record and tectonic implications of Mesozoic rifting in southeast Mongolia. Bull Geol Soc Am 113:1560–1579.
Groth E, K Tandre, P Engström, F Vergara-Silva 2011 AGAMOUS subfamily MADS-box genes and the evolution of seed cone morphology in Cupressaceae and Taxodiaceae. Evol Dev 13:159–170.
Guédès M, P Dupuy 1971 Morphology of the seed-scale complex in *Pinus pinaster* subsp. *atlantica*: a teratologic approach. Phytomorphology 21:17–31.
——— 1974 Morphology of the seed-scale complex in *Picea abies* (L.) Karst. (Pinaceae). Bot J Linn Soc 68:127–141.
Hernandez-Castillo GR, RA Stockey, GW Rothwell, G Mapes 2009 Reconstructing *Emporia lockardii* (Voltziales: Emporiaceae) and initial thoughts on Paleozoic conifer ecology. Int J Plant Sci 170:1056–1074.
Herrera F, AB Leslie, G Shi, P Knopf, N Ichinnorov, M Takahashi, PR Crane, PS Herendeen 2016 New fossil Pinaceae from the Early Cretaceous of Mongolia. Botany 94:885–915.
Herrera F, G Shi, P Knopf, AB Leslie, N Ichinnorov, M Takahashi, PR Crane, PS Herendeen 2017 Cupressaceae conifers from the Early Cretaceous of Mongolia. Int J Plant Sci 178:19–41.
Herrera F, G Shi, AB Leslie, P Knopf, N Ichinnorov, M Takahashi, PR Crane, PS Herendeen 2015 A new voltzian seed cone from the Early Cretaceous of Mongolia and its implications for the evolution of ancient conifers. Int J Plant Sci 176:791–809.
Herrera F, G Shi, C Mays, N Ichinnorov, M Takahashi, JJ Bevitt, PS Herendeen, PR Crane 2020 Reconstructing *Krassilovia mongolica* supports recognition of a new and unusual group of Mesozoic conifers. PLoS ONE 15:1–21.
Ichinnorov N 2003 Palynocomplex of the Lower Cretaceous sediments of eastern Mongolia. Mong Geosci 22:12–16.
——— 2005 Pollen and spore assemblages and their stratigraphic significance. Mong Geosci 24:160–162.
Jagel A, VM Dörken 2014 Morphology and morphogenesis of the seed cones of the Cupressaceae. I. Cunninghamioideae, Athrotaxoideae, Taiwanioideae, Sequoioideae, Taxodioideae. Bull Cupressus Conserv Proj 3:117–136.
——— 2015*a* Morphology and morphogenesis of the seed cones of the Cupressaceae. II. Cupressoideae. Bull Cupressus Conserv Proj 4:51–78.
——— 2015*b* Morphology and morphogenesis of the seed cones of the Cupressaceae. III. Callitroideae. Bull Cupressus Conserv Proj 4:91–108.
Joy KW, AJ Willis, WS Lacey 1956 A rapid cellulose peel technique in palaeobotany. Ann Bot 20:635–637.
Katoh K, DM Standley 2013 MAFFT multiple sequence alignment software version 7: improvements in performance and usability. Mol Biol Evol 30:772–80.
Klymiuk AA, RA Stockey 2012 A Lower Cretaceous (Valanginian) seed cone provides the earliest fossil record for *Picea* (Pinaceae). Am J Bot 99:1069–1082.
Lanfear R, B Calcott, SYW Ho, S Guindon 2012 PartitionFinder: combined selection of partitioning schemes and substitution models for phylogenetic analyses. Mol Biol Evol 29:1695–1701.
Lanfear R, PB Frandsen, AM Wright, T Senfeld, B Calcott 2017 Partitionfinder 2: new methods for selecting partitioned models of evolution for molecular and morphological phylogenetic analyses. Mol Biol Evol 34:772–773.
Leslie AB 2010 Flotation preferentially selects saccate pollen during conifer pollination. New Phytol 188:273–279.
Leslie AB, J Beaulieu, G Holman, CS Campbell, W Mei, LR Raubeson, S Mathews 2018 An overview of extant conifer evolution from the perspective of the fossil record. Am J Bot 105:1531–1544.
Leslie AB, I Glasspool, PS Herendeen, N Ichinnorov, P Knopf, M Takahashi, PR Crane 2013 Pinaceae-like reproductive morphology in *Schizolepidopsis canicularis* sp. nov. from the Early Cretaceous (Aptian-Albian) of Mongolia. Am J Bot 100:2426–2436.
Li R, X Wang, P Jin, M Fujun, D Yan, L Zhicheng, B Sun 2016 Fossil liverworts from the Lower Cretaceous Huolinhe Formation in Inner Mongolia, China. Acta Geol Sin 90:838–846.
Looy CV 2007 Extending the range of derived Late Paleozoic conifers: *Lebowskia* gen. nov. (Majonicaceae). Int J Plant Sci 168:957–972.
Mapes G, GW Rothwell 1984 Permineralized ovulate cones of Lebachia from late Paleozoic limestones of Kansas. Paleontology 27:69–94.
——— 2003 Validation of the names Emporiaceae, *Emporia*, and *Emporia lockardii*. Taxon 52:327–328.
Meyen SV 1987 Fundamentals of palaeobotany. Chapman & Hall, London.
Mill RR, M Möller, F Christie, SM Glidewell, D Masson, B Williamson 2001 Morphology, anatomy and ontogeny of female cones in *Acmopyle pancheri* (Brongn. & Gris) Pilg. (Podocarpaceae). Ann Bot 88:55–67.
Miller CN 1976 Early evolution in the Pinaceae. Rev Palaeobot Palynol 21:101–117.
Miller MA, W Pfeiffer, T Schwartz 2010 Creating the CIPRES Science Gateway for inference of large phylogenetic trees. Pages 1–8 *in* 2010

Gateway Computing Environments Workshop. Institute of Electrical and Electronics Engineers, New York.

Owens JN, MD Blake 1983 Pollen morphology and development of the pollination mechanism in *Tsuga heterophylla* and *T. mertensiana*. Can J Bot 61:3041–3048.

Owens JN, GL Catalano, SJ Morris, J Aitken-Christie 1995 The reproductive biology of Kauri (*Agathis australis*). I. Pollination and prefertilization development. Int J Plant Sci 156:257–269.

Owens JN, T Takaso, CJ Runions 1998 Pollination in conifers. Trends Plant Sci 3:479–485.

Radais M 1894 Contribution a l'anatomie comparée du fruit des coniféres. Académie de Paris, Paris.

Rothwell GW 1993 *Cordaixylon dumusum* (Cordaitales). II. Reproductive biology, phenology, and growth ecology. Int J Plant Sci 154:572–586.

Rothwell GW, G Mapes, GR Hernandez-Castillo 2005 *Hanskerpia* gen. nov. and phylogenetic relationships among the most ancient conifers (Voltziales). Taxon 54:733–750.

Rothwell GW, G Mapes, RA Stockey, J Hilton 2012 The seed cone *Eathiestrobus* gen. nov.: fossil evidence for a Jurassic origin of Pinaceae. Am J Bot 99:708–720.

Rothwell GW, RA Stockey, G Mapes, J Hilton 2011 Structure and relationships of the Jurassic conifer seed cone *Hughmillerites juddii* gen. et comb. nov.: implications for the origin and evolution of Cupressaceae. Rev Palaeobot Palynol 164:45–59.

Ruelens P, K Geuten 2013 When paleontology and molecular genetics meet: a genetic context for the evolution of conifer ovuliferous scales. New Phytol 200:10–12.

Runions CJ, GL Catalano, JN Owens 1995 Pollination mechanism of seed orchard interior spruce. Can J For Res 25:1434–1444.

Ryberg PE, GW Rothwell, RA Stockey, J Hilton, G Mapes, JB Riding 2012 Reconsidering relationships among stem and crown group Pinaceae: oldest record of the genus *Pinus* from the Early Cretaceous of Yorkshire, United Kingdom. Int J Plant Sci 173:917–932.

Schulz C, T Stützel 2007 Evolution of taxodiaceous Cupressaceae (Coniferopsida). Org Divers Evol 7:124–135.

Shi G, AB Leslie, PS Herendeen, N Ichinnorov, M Takahashi, P Knopf, PR Crane 2014 Whole-plant reconstruction and phylogenetic relationships of *Elatides zhoui* sp. nov. (Cupressaceae) from the Early Cretaceous of Mongolia. Int J Plant Sci 175:911–930.

Smith SY, RA Stockey 2001 A new species of *Pityostrobus* from the Lower Cretaceous of California and its bearing on the evolution of Pinaceae. Int J Plant Sci 162:669–681.

Smith SY, RA Stockey, GW Rothwell, SA Little 2016 A new species of *Pityostrobus* (Pinaceae) from the Cretaceous of California: moving towards understanding the Cretaceous radiation of Pinaceae. J Syst Palaeontol 15:69–81.

Spencer ART, G Mapes, RM Bateman, J Hilton, GW Rothwell 2015 Middle Jurassic evidence for the origin of Cupressaceae: a paleobotanical context for the roles of regulatory genetics and development in the evolution of conifer seed cones. Am J Bot 102:942–961.

Stamatakis A 2014 RAxML version 8: a tool for phylogenetic analysis and post-analysis of large phylogenies. Bioinformatics 30:1312–1313.

Stewart WN, GW Rothwell 1993 Paleobotany and the evolution of plants. 2nd ed. Cambridge University Press, Cambridge.

Stockey RA 1982 The Araucariaceae: an evolutionary perspective. Rev Palaeobot Palynol 37:133–154.

Swofford DL 2003 PAUP*: phylogenetic analysis using parsimony (*and other methods). http://paup.phylosolutions.com/.

Takaso T, JN Owens 1995 Ovulate cone morphology and pollination in *Pseudotsuga* and *Cedrus*. Int J Plant Sci 156:630–639.

Takaso T, PB Tomlinson 1989 Aspects of cone and ovule ontogeny in *Cryptomeria* (Taxodiaceae). Am J Bot 76:692–705.

——— 1991 Cone and ovule development in *Sciadopitys* (Taxodiaceae-Coniferales). Am J Bot 78:417–428.

——— 1992 Seed cone and ovule ontogeny in *Metasequoia*, *Sequoia* and *Sequoiadendron* (Taxodiaceae-Coniferales). Bot J Linn Soc 109: 15–37.

Taylor EL, TN Taylor, MM Krings 2009 Paleobotany: the biology and evolution of fossil plants. Academic Press, Amsterdam.

Tomlinson PB 1992 Aspects of cone morphology and development in Podocarpaceae (Coniferales). Int J Plant Sci 153:572–588.

Tomlinson PB, JE Braggins, JA Rattenbury 1991 Pollination drop in relation to cone morphology in Podocarpaceae: a novel reproductive mechanism. Am J Bot 78:1289–1303.

Tomlinson PB, T Takaso 1989 Cone and ovule ontogeny in *Phyllocladus* (Podocarpaceae). Bot J Linn Soc 99:209–221.

Wang X, S Duan, J Cui 1997 Several species of *Schizolepis* and their significance on the evolution of conifers. Taiwania 42:73–85.

Xu X, R Li, C Dong, Q Wang, P Jin, B Sun 2013 New *Schizolepis* fossils from the Early Cretaceous in Inner Mongolia, China and its phylogenetic position. Acta Geol Sin 87:1250–1263.

Yao X, TN Taylor, EL Taylor 1997 A taxodiaceous seed cone from the Triassic of Antarctica. Am J Bot 84:343–354.

Zhang J, A D'Rozario, J Yao, Z Wu, L Wang 2011 A new species of the extinct genus *Schizolepis* from the Jurassic Daohugou flora, Inner Mongolia, China, with special reference to the fossil diversity and evolutionary implications. Acta Geol Sin 85:471–481.